Electromagnetic scattering of an arbitrary plane wave from a spherical shell with a circular aperture

Richard W. Ziolkowski
Electronics Engineering Department, Lawrence Livermore National Laboratory, P.O. Box 5504, L-156, Livermore, California 94550

William A. Johnson[a)]
Division 7553, Sandia National Laboratories, Albuquerque, New Mexico 87185

(Received 23 July 1985; accepted for publication 30 January 1987)

The problem of the scattering of an electromagnetic plane wave with arbitrary polarization and angle of incidence from a perfectly conducting spherical shell with a circular aperture is solved with a generalized dual series approach. This canonical problem encompasses coupling to an open spherical cavity and scattering from a spherical reflector. In contrast to the closed sphere problem, the electromagnetic boundary conditions couple the TE and TM modes. A pseudodecoupling of the resultant dual series equations system into dual series problems for the TE and TM modal coefficients is accomplished by introducing terms that are proportional to the associated Legendre functions P_0^{-m}. The solutions of the TE and TM dual series problems require the further introduction of terms proportional to P_n^{-m}, where $0 \leqslant n < m$. These functions effectively complete the standard spherical harmonic basis set when an aperture is present and guarantee the satisfaction of Meixner's edge conditions. Having generated the modal coefficients, all desired electromagnetic quantities follow immediately. Numerical results for the currents induced on the open spherical shell and for the energy density of the field at its center are presented for the case of normal incidence.

I. INTRODUCTION

The number of electromagnetic boundary value problems that can be solved exactly is rather small, especially in three dimensions. The desire and the need for these canonical problems, however, is very strong. They reveal the basic physics underlying the phenomena and help establish insights that can usually be extrapolated to more general situations. Moreover, they act as valuable test cases for general numerical approaches to related problems.

The scattering of an electromagnetic plane wave from a perfectly conducting closed sphere is probably the best known three-dimensional canonical scattering problem. Its generalization, the scattering of a plane wave from a perfectly conducting spherical shell with a circular aperture, is important from both theoretical and practical points of view. In particular, when the circular hole has a relatively small angular extent, this problem allows one to study the coupling of a wave from an external source through an aperture into an enclosed region. On the other hand, when the shell has a relatively small angular extent, the problem describes the scattering of a plane wave from a spherical reflector. A complete solution to this canonical mixed boundary value problem is given in this paper.

A Debye potential formulation is employed, but in contrast to standard treatments in spherical geometries, the associated Legendre polynomials of negative order (P_n^{-m}, $n \geqslant m$) are utilized for the modal expansions. Enforcement of the electromagnetic boundary conditions leads to a coupled set of dual series equations for the TE and TM modal coefficients of each azimuthal mode. A pseudodecoupling ansatz is developed to allow separate treatment of the TE and TM dual series systems. It requires the introduction of terms proportional to the associated Legendre polynomials P_0^{-m} (m being the azimuthal mode number) which are homogeneous solutions of the boundary condition equations. Solutions of the resulting "uncoupled" TE and TM dual series systems are given. They require the further introduction of terms proportional to the associated Legendre polynomials whose degree is less than its order: P_n^{-m}, where $0 \leqslant n < m$. These terms guarantee satisfaction of Meixner's edge conditions and effectively complete the spherical harmonic basis set in the presence of the aperture. Infinite systems of Fredholm equations of the second kind for the modal coefficients are obtained. A rigorous truncation procedure is given that leads to a straightforward numerical evaluation of those coefficients. Results for the currents induced on the open spherical shell and for an energy density ratio as a function of the fundamental parameter ka ($2\pi \times$ radius/wavelength) are presented for the case of normal incidence. It is shown analytically that the behavior of the currents near the edge of the aperture are in agreement with Meixner's edge conditions; the graphical results further confirm this. The energy density scans highlight the resonance features of the coupling physics.

This paper is organized as follows. In Sec. II the coupled dual series systems are derived for the scattering of a general plane wave from an open spherical shell. The decoupling ansatz is presented is Sec. III, and the resulting TE and TM dual series systems are solved in Sec. IV. The results are then restricted to the normal incidence case in Sec. V. In Sec. VI the currents induced on the open spherical shell are given for various values of ka, aperture size, and the two allowed angles of incidence. Their modal structure is exhibited with a set of three-dimensional color figures. The energy density scans are discussed in Sec. VII.

[a)] Present address: Division 1265, Sandia National Laboratories, Albuquerque, New Mexico 87185.

Downloaded 21 Nov 2006 to 150.135.222.53. Redistribution subject to AIP license or copyright, see http://jmp.aip.org/jmp/copyright.jsp

There have been several reports of solutions to the normally incident case of the open spherical shell problem from both analytical[1–10] and numerical[11–15] points of view. In the numerical papers, various convergence problems and erroneous results are encountered. Of the analytical papers only Ref. 9 seems to lead to correct results for the scattering problem. Unfortunately, direct comparisons for that case are difficult because the dual series systems and their solutions (which were checked with our validation scheme) differ from those obtained here and no current or field values were calculated there. Moreover, the basic tenets of Ref. 9 appear to be restricted to the normal incidence case. The errors in Refs. 1–8 and 10 are either that the dual series systems were solved incorrectly or, more fundamentally, that the wrong dual series systems were solved. The latter stems from the erroneous assumption that the TE and TM dual series are completely decoupled. This error is identical to the one made by Meixner in his original Debye potential solution to the scattering of a plane wave from a circular hole in a perfectly conducting ground plane.[16] In analogy with our approach, Meixner corrected that error in Ref. 17 by introducing additional potentials that were homogeneous solutions of the equations resulting from enforcement of the electromagnetic boundary conditions. The coefficients of these potentials were chosen to guarantee that the fields satisfy the correct edge behavior, hence accounting for the presence of the aperture. The pseudodecoupling ansatz can be shown to be equivalent to a gauge transformation, which in analogy with Dirac string analyses, involves discontinuous potentials, the gauge conditions being identical to the pseudodecoupling constraint conditions.[18]

The results for normal incidence were closely compared with those generated with a general, numerical surface patch scattering code; and these comparisons were reported in Ref. 19. The agreement is excellent; and since that code has been validated with a variety of different scattering problems, this lends further credence to the validity of the solution presented below. The present work represents a generalization of related aperture coupling work[20–24] to three dimensions. A more detailed presentation is available.[25] It includes many complementary results that were omitted here simply because of length considerations.

II. REDUCTION TO COUPLED DUAL SERIES PROBLEM

Consider the problem configuration shown in Fig. 1. A perfectly conducting open thin spherical shell is represented by the surface $r = a$, $0 \leqslant \theta < \theta_0$ in the spherical coordinate system (r,θ,ϕ) erected at the shell's center. The negative z axis of that system passes through the center of the aperture, the latter being defined as $\{(r,\theta,\phi) | r = a \text{ and } \theta_0 < \theta \leqslant \pi\}$. The opening angle of the aperture, θ_{ap}, is defined simply as $\theta_{ap} = \pi - \theta_0$. The medium inside and outside the shell is free space. The unit vectors $(\hat{r},\hat{\theta},\hat{\phi})$ are defined in the standard manner in the directions of positively increasing coordinate values.

Mathematically, we are seeking, for an arbitrary incident plane wave, the field scattered by the open spherical shell. This scattered field must satisfy the Sommerfeld radiation condition as $r \to \infty$. The total field (incident + scattered) must satisfy (1) the electromagnetic conditions, $E_{tan} = 0$ on the metallic shell and H_{tan} continuous over the aperture; and (2) Meixner's edge conditions,[17,26] i.e., the total energy of the field must be finite near the aperture rim.

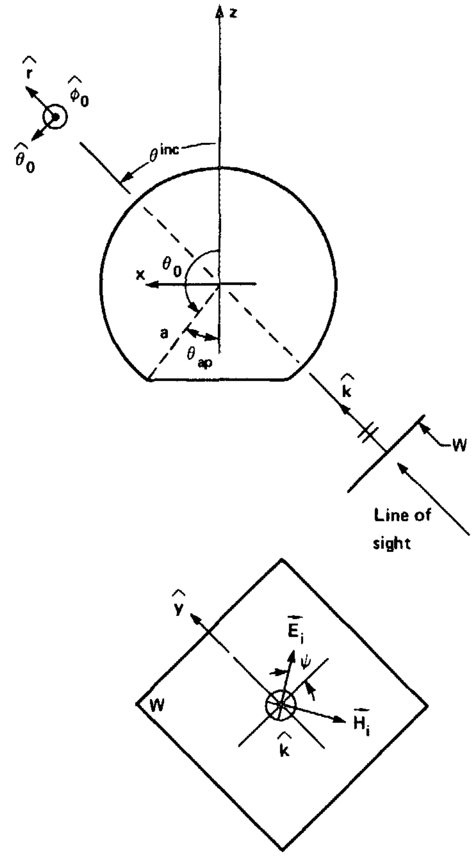

FIG. 1. Configuration of the scattering of an arbitrary plane wave from a spherical shell having a circular aperture.

A. Debye expansions

A plane wave with electric field strength E_0 is incident on the open spherical shell. It is characterized by a wave vector $\mathbf{k}$, which for convenience is assumed to lie in the xz plane; an incident angle θ^{inc} with respect to the z axis so that $\mathbf{k}\cdot\hat{z} = \cos\theta^{inc}$; and a polarization angle ψ between $\mathbf{E}$ and the projection of the positive z axis on the incident wave front. The incident field has the form

$$\begin{bmatrix} \mathbf{E}^{inc} \\ Z_0\mathbf{H}^{inc} \end{bmatrix} = -E_0 e^{i\mathbf{k}\cdot\mathbf{r}} \begin{bmatrix} (\cos\psi)\hat{\theta}_0 - (\sin\psi)\hat{\phi}_0 \\ (\sin\psi)\hat{\theta}_0 + (\cos\psi)\hat{\phi}_0 \end{bmatrix}, \quad (2.1)$$

where $\hat{\theta}_0$ and $\hat{\phi}_0$ are the incident polarization vectors and where, as throughout this paper, an $e^{-i\omega t}$ time dependence has been assumed and suppressed. The free-space impedance Z_0 is related to the free-space admittance $Y_0 = (\epsilon/\mu)^{1/2}$ as $Z_0 = Y_0^{-1}$ and the wave number $k = \omega(\epsilon\mu)^{1/2}$, where ϵ and μ denote, respectively, the permittivity and permeability of free space. The incident field parameters are indicated in Fig. 1. The incident electric field is polarized perpendicular to the edge of the aperture when $\psi = 0$ and is polarized parallel to it when $\psi = \pi/2$. Since any incident plane wave can be reduced to a linear superposition of these waves, only they

Downloaded 21 Nov 2006 to 150.135.222.53. Redistribution subject to AIP license or copyright, see http://jmp.aip.org/jmp/copyright.jsp

TABLE I. The electric and magnetic field components in spherical coordinates in terms of Debye potentials.

$E_r = -\frac{1}{i\omega\epsilon}\left\{\frac{\partial^2}{\partial r^2} + k^2\right\}(r\Psi)$
$E_\theta = -\frac{1}{r\sin\theta}\frac{\partial}{\partial\phi}(r\Phi) - \frac{1}{(i\omega\epsilon)r}\frac{\partial^2}{\partial r\,\partial\theta}(r\Psi)$
$E_\phi = \frac{1}{r}\frac{\partial}{\partial\theta}(r\Phi) - \frac{1}{(i\omega\epsilon)r\sin\theta}\frac{\partial^2}{\partial r\,\partial\phi}(r\Psi)$
$H_r = -\frac{1}{i\omega\mu}\left\{\frac{\partial^2}{\partial r^2} + k^2\right\}(r\Phi)$
$H_\theta = \frac{1}{r\sin\theta}\frac{\partial}{\partial\phi}(r\Psi) - \frac{1}{(i\omega\mu)r}\frac{\partial^2}{\partial r\,\partial\theta}(r\Phi)$
$H_\phi = -\frac{1}{r}\frac{\partial}{\partial\theta}(r\Psi) - \frac{1}{(i\omega\mu)r\sin\theta}\frac{\partial^2}{\partial r\,\partial\phi}(r\Phi)$

need to be addressed explicitly. Moreover, with the intrinsic symmetry of the field components in Maxwell's equations, the $\psi = \pi/2$ case is readily obtained from the $\psi = 0$ case. Consequently, we restrict our considerations to the $\psi = 0$ case with no loss in generality.

Following standard analyses of problems in a spherically symmetric geometry, we employ a Debye potential formalism.[27–29] In particular, the electric and magnetic fields are expressed in terms of the two vector potentials $\Phi\mathbf{r}$ and $\Psi\mathbf{r}$ as

$$\mathbf{E} = -\operatorname{curl}(\Phi\mathbf{r}) - (i\omega\epsilon)^{-1}\operatorname{curl}\operatorname{curl}(\Psi\mathbf{r}), \tag{2.2}$$

$$\mathbf{H} = +\operatorname{curl}(\Psi\mathbf{r}) - (i\omega\mu)^{-1}\operatorname{curl}\operatorname{curl}(\Phi\mathbf{r}), \tag{2.3}$$

where the radial vector $\mathbf{r} = r\hat{r}$. Their components are given explicitly in Table I. The scalar functions Φ and Ψ may represent any combination of the incident and scattered fields. The function Φ defines the field TE with respect to r, Ψ the field TM with respect to r. The descriptor "with respect to r" is assumed and suppressed throughout the rest of this paper.

The spherical wave expansion of the incident field (2.1) with $\psi = 0$ given, for instance, in Ref. 30 or Ref. 31, can be generated with the Debye scalar potentials, $\Phi^{\rm inc}$ and $\Psi^{\rm inc}$, defined below. Since the scattered potentials, Φ^s and Ψ^s, assume an analogous form, we have

$$\begin{pmatrix}\Phi^{\rm inc}\\ \Phi^s\end{pmatrix} = -E_0\sum_{m=0}^{\infty}\begin{pmatrix}\Phi_m^{\rm inc}\\ \Phi_m^s\end{pmatrix}\sin m\phi, \tag{2.4}$$

$$\begin{pmatrix}\Psi^{\rm inc}\\ \Psi^s\end{pmatrix} = Y_0E_0\sum_{m=0}^{\infty}\begin{pmatrix}\Psi_m^{\rm inc}\\ \Psi_m^s\end{pmatrix}\cos m\phi, \tag{2.5}$$

where the azimuthal modal coefficients

$$\Phi_m^{\rm inc} = \sum_{n=m}^{\infty}\gamma_{mn}\left[\frac{mP_n^m(\cos\theta^{\rm inc})}{\sin\theta^{\rm inc}}\right]j_n(kr)P_n^{-m}(\cos\theta), \tag{2.6}$$

$$\Psi_m^{\rm inc} = \sum_{n=m}^{\infty}\gamma_{mn}\left[-\left(\frac{\partial}{\partial\theta}P_n^m\right)(\cos\theta^{\rm inc})\right] \times j_n(kr)P_n^{-m}(\cos\theta), \tag{2.7}$$

$$\Phi_m^s = \sum_{n=m}^{\infty}A_{mn}P_n^{-m}(\cos\theta)\begin{cases}j_n(kr)h_n(ka) & (r<a),\\ j_n(ka)h_n(kr) & (r>a),\end{cases} \tag{2.8}$$

$$\Psi_m^s = \sum_{n=m}^{\infty}B_{mn}P_n^{-m}(\cos\theta) \times\begin{cases}j_n(kr)[kah_n(ka)]' & (r<a),\\ [kaj_n(ka)]'h_n(kr) & (r>a),\end{cases} \tag{2.9}$$

where

$$\gamma_{mn} = (-1)^{m+1}i^n[(2n+1)/n(n+1)]\epsilon_m(1-\delta_{0n}). \tag{2.10}$$

The terms j_n and h_n are, respectively, the spherical Bessel and Hankel (of the first kind) functions of order n. The associated Legendre polynomials of degree n, order $\pm m$, are denoted by $P_n^{\pm m}$. The prime in an expression $[xf_n(x)]'$ denotes the derivative with respect to x. The term $\epsilon_m = 2$ for $m \neq 0$ and $\epsilon_m = 1$ for $m = 0$. Kronecker's delta $\delta_{ij} = 0$ for $i \neq j$ and $\delta_{jj} = 1$ for any j. Because the term corresponding to both $m = 0$ and $n = 0$ is identically zero in the incident field, we set the corresponding scattered potential coefficients identically to zero: $A_{00} \equiv B_{00} \equiv 0$.

These representations of the interior and exterior scattered potentials have been chosen so that Φ^s and $\partial_r(r\Psi^s)$ are continuous at $r = a$, thereby ensuring the continuity of the tangential scattered electric field components E_θ and E_ϕ across that surface. The resultant fields satisfy Sommerfeld's radiation condition; the dependence of the scattered fields on $h_n(kr)$ for $r > a$ ensures their decay to zero as $r \to \infty$. The modal coefficients A_{mn} and B_{mn} are the quantities that must be determined.

B. Electromagnetic boundary conditions

The electromagnetic boundary conditions: $E_{\rm tan} = 0$ on the metal and $H_{\rm tan}$ continuous in the aperture, are now enforced. Referring to Table I, $E_\theta = 0$ on the metal if

$$\sum_{m=0}^{\infty}\cos m\phi\left\{\frac{m}{\sin\theta}(\Phi_m^{\rm inc} + \Phi_m^s) - \frac{Y_0}{i\omega\epsilon}\frac{1}{r}\frac{\partial^2}{\partial r\,\partial\theta}[r(\Psi_m^{\rm inc} + \Psi_m^s)]\right\}_{r=a} = 0,$$

$E_\phi = 0$ on the metal if

$$\sum_{m=0}^{\infty}\sin m\phi\left\{-\frac{\partial}{\partial\theta}(\Phi_m^{\rm inc} + \Phi_m^s) + \frac{Y_0}{i\omega\epsilon}\frac{m}{r\sin\theta}\frac{\partial}{\partial r}[r(\Psi_m^{\rm inc} + \Psi_m^s)]\right\}_{r=a} = 0,$$

H_θ is continuous across the aperture if for $\epsilon \to 0$

$$\sum_{m=0}^{\infty}\sin m\phi\left\{\frac{-mY_0}{\sin\theta}(\Psi_m^{\rm inc} + \Psi_m^s) + \frac{1}{i\omega\mu}\frac{1}{r}\frac{\partial^2}{\partial r\,\partial\theta}[r(\Phi_m^{\rm inc} + \Phi_m^s)]\right\}_{r=a-\epsilon}^{r=a+\epsilon} = 0,$$

and H_ϕ is continuous across the aperture if for $\epsilon \to 0$

$$\sum_{m=0}^{\infty}\cos m\phi\left\{-Y_0\frac{\partial}{\partial\theta}(\Psi_m^{\rm inc} + \Psi_m^s) + \frac{1}{i\omega\mu}\frac{m}{r\sin\theta}\frac{\partial}{\partial r}[r(\Phi_m^{\rm inc} + \Phi_m^s)]\right\}_{r=a-\epsilon}^{r=a+\epsilon} = 0.$$

Because the azimuthal eigenfunctions $\sin m\phi$ and $\cos m\phi$ form an orthogonal set over $[0,2\pi]$, these conditions must be satisfied on a mode by mode basis. They require satisfac-

Downloaded 21 Nov 2006 to 150.135.222.53. Redistribution subject to AIP license or copyright, see http://jmp.aip.org/jmp/copyright.jsp

tion of the following coupled set of dual series equations for the modal coefficients A_{mn} and B_{mn}:

$$ika \sum_{n=m}^{\infty} \{A_{mn} j_n(ka) h_n(ka) - f_{mn}\} m P_n^{-m}(\cos\theta)$$

$$= \sin\theta\,\partial_\theta \sum_{n=m}^{\infty} \{B_{mn}[kaj_n(ka)]'[kah_n(ka)]' - g_{mn}\} P_n^{-m}(\cos\theta) \quad (0 \leqslant \theta < \theta_0), \tag{2.11a}$$

$$\sum_{n=m}^{\infty} A_{mn} m P_n^{-m}(\cos\theta) = -ika \sin\theta\,\partial_\theta \sum_{n=m}^{\infty} B_{mn} P_n^{-m}(\cos\theta) \quad (\theta_0 < \theta \leqslant \pi), \tag{2.11b}$$

$$ika \sin\theta\,\partial_\theta \sum_{n=m}^{\infty} \{A_{mn} j_n(ka) h_n(ka) - f_{mn}\} P_n^{-m}(\cos\theta)$$

$$= \sum_{n=m}^{\infty} \{B_{mn}[kaj_n(ka)]'[kah_n(ka)]' - g_{mn}\} m P_n^{-m}(\cos\theta) \quad (0 \leqslant \theta < \theta_0), \tag{2.12a}$$

$$\sin\theta\,\partial_\theta \sum_{n=m}^{\infty} A_{mn} P_n^{-m}(\cos\theta) = -ika \sum_{n=m}^{\infty} B_{mn} m P_n^{-m}(\cos\theta) \quad (\theta_0 < \theta \leqslant \pi), \tag{2.12b}$$

where

$$f_{mn} = \gamma_{mn} [m P_n^m(\cos\theta^{\rm inc})/\sin\theta^{\rm inc}] j_n(ka), \tag{2.13}$$

$$g_{mn} = \gamma_{mn} \left[\left(\frac{\partial}{\partial\theta} P_n^m\right)(\cos\theta^{\rm inc})\right][kaj_n(ka)]'. \tag{2.14}$$

Equations (2.11) result from the E_θ and H_ϕ boundary conditions and are naturally paired because their θ and ϕ dependencies are the same; Eqs. (2.12) result from the E_ϕ and H_θ boundary conditions. The absence of any spherical Bessel or Hankel function in (2.11b) and (2.12b) results from application of the modified Wronskian relation

$$j_n(x)[xh_n(x)]' - h_n(x)[xj_n(x)]' = i/x. \tag{2.15}$$

Note that $\partial_\theta \equiv \partial/\partial\theta$.

III. PSEUDODECOUPLING ANSATZ

In the problem of plane wave scattering from a solid sphere it is known[27] that the TE and TM portions of the problem may be decoupled. Satisfaction of independent boundary conditions applied directly to the TE and TM Debye potentials leads to series defined over the entire θ interval, $[0,\pi]$; and orthogonality arguments then produce a complete decoupling. Introducing the hole results in mixed boundary conditions over partial θ intervals and a coupling of the TE and TM modes. Nonetheless, one might anticipate some form of TE/TM decoupling even in this case if the proper set of basis functions were employed.

Consider the associated Legendre functions of negative order $P_n^{-m}(\cos\theta)$. For all n and m they are known independent solutions to Legendre's equation[32-35]:

$$\mathscr{L}_\theta P_n^{-m}(\cos\theta) = -n(n+1)(\sin^2\theta) P_n^{-m}(\cos\theta), \tag{3.1}$$

where the operator

$$\mathscr{L}_\theta \equiv (\sin\theta\,\partial_\theta)(\sin\theta\,\partial_\theta) - m^2. \tag{3.2}$$

They have the integral representations[32]

$$P_n^{-m}(\cos\theta) = (-1)^m \left(\frac{2}{\pi}\right)^{1/2} \frac{\csc^m\theta}{\Gamma(m+\frac{1}{2})} \times \int_0^\theta \frac{\cos[(n+\frac{1}{2})t]\,dt}{[\cos t - \cos\theta]^{1/2-m}}. \tag{3.3}$$

Note that our definition of P_n^{-m} differs from that in Ref. 32 by the factor $(-1)^m$. The related functions

$$\bar{P}_n^{-m}(\cos\theta) \equiv (-1)^{n+m} P_n^{-m}(\cos(\pi-\theta)) = (-1)^m \left(\frac{2}{\pi}\right)^{1/2} \frac{\csc^m\theta}{\Gamma(m+\frac{1}{2})} \times \int_\theta^\pi \frac{\sin[(n+\frac{1}{2})t]\,dt}{[\cos\theta - \cos t]^{1/2-m}} \tag{3.4}$$

also satisfy (3.1). For $n \geqslant m$, these functions are identical by the standard symmetry relation

$$\bar{P}_n^{-m}(\cos\theta) \equiv (-1)^{n+m} P_n^{-m}(\cos(\pi-\theta)) \equiv P_n^{-m}(\cos\theta). \tag{3.5}$$

However, for $0 \leqslant n < m$, this relation no longer holds true. In particular, $P_n^{-m}(\cos\theta)$ is finite at $\theta = 0$ but infinite at $\theta = \pi$. On the other hand, $\bar{P}_n^{-m}(\cos\theta)$ is finite at $\theta = \pi$ but infinite at $\theta = 0$. This behavior is immediately apparent for $n = 0$ where

$$P_0^{-m}(\cos\theta) = [(-1)^m/m!] \tan^m(\theta/2), \tag{3.6a}$$

$$\bar{P}_0^{-m}(\cos\theta) = (1/m!) \cot^m(\theta/2). \tag{3.6b}$$

Return now to the dual series systems (2.11) and (2.12). They are self-consistent if

$$\left.\begin{aligned} &\mathscr{L}_\theta \sum_{n=m}^{\infty} \{A_{mn} j_n(ka) h_n(ka) - f_{mn}\} P_n^{-m}(\cos\theta) = 0 \\ &\mathscr{L}_\theta \sum_{n=m}^{\infty} \{B_{mn}[kaj_n(ka)]'[kah_n(ka)]' - g_{mn}\} P_n^{-m}(\cos\theta) = 0 \end{aligned}\right\} \quad (0 \leqslant \theta < \theta_0);$$

Downloaded 21 Nov 2006 to 150.135.222.53. Redistribution subject to AIP license or copyright, see http://jmp.aip.org/jmp/copyright.jsp

$$\mathscr{L}_\theta \sum_{n=m}^{\infty} A_{mn} P_n^{-m}(\cos\theta) = 0$$
$$(\theta_0 < \theta \leqslant \pi).$$
$$\mathscr{L}_\theta \sum_{n=m}^{\infty} B_{mn} P_n^{-m}(\cos\theta) = 0$$

Bounded homogeneous solutions of these equations are admissible and are proportional to $P_0^{-m}(\cos\theta)$ and $\overline{P}_0^{-m}(\cos\theta)$ over their respective intervals. Solutions to the TE dual series system

$$\sum_{n=m}^{\infty} \{A_{mn} j_n(ka) h_n(ka) - f_{mn}\} P_n^{-m}(\cos\theta)$$
$$= \alpha_m P_0^{-m}(\cos\theta) \quad (0 \leqslant \theta < \theta_0), \tag{3.7a}$$

$$\sum_{n=m}^{\infty} A_{mn} P_n^{-m}(\cos\theta) = \overline{\alpha}_m \overline{P}_0^{-m}(\cos\theta) \quad (\theta_0 < \theta \leqslant \pi), \tag{3.7b}$$

for $m \geqslant 1$ and to the TM dual series system

$$\sum_{n=m}^{\infty} \{B_{mn}[kaj_n(ka)]'[kah_n(ka)]' - g_{mn}\} P_n^{-m}(\cos\theta)$$
$$= \beta_m P_0^{-m}(\cos\theta) \quad (0 \leqslant \theta < \theta_0), \tag{3.8a}$$

$$\sum_{n=m}^{\infty} B_{mn} P_n^{-m}(\cos\theta) = \overline{\beta}_m \overline{P}_0^{-m}(\cos\theta) \quad (\theta_0 < \theta \leqslant \pi), \tag{3.8b}$$

for $m \geqslant 0$ are therefore solutions to (2.11) and (2.12) provided that the "decoupling" constants α_m, β_m, $\overline{\alpha}_m$, and $\overline{\beta}_m$ are constrained by those coupled dual series equations. Since

$$\sin\theta\, \partial_\theta \begin{bmatrix} P_0^{-m}(\cos\theta) \\ \overline{P}_0^{-m}(\cos\theta) \end{bmatrix} = m \begin{bmatrix} +P_0^{-m}(\cos\theta) \\ -\overline{P}_0^{-m}(\cos\theta) \end{bmatrix}, \tag{3.9}$$

the required constraint relations for $m \geqslant 1$ are simply

$$\beta_m = ika\alpha_m, \tag{3.10}$$
$$\overline{\alpha}_m = ika\overline{\beta}_m. \tag{3.11}$$

There is no $m = 0$ constraint relation because there is no $m = 0$ TE dual series equation.

Consequently, although the TE and TM portions of the dual series systems (2.11) and (2.12) have been decoupled, the TE and TM modal coefficients are still coupled through these "decoupling" constant constraint relations. This explains the connotation "pseudodecoupling ansatz." The solutions to the TE and TM dual series systems (3.7) and (3.8) subject to the constraints (3.10) and (3.11) comprise the desired result.

IV. TE AND TM DUAL SERIES SOLUTIONS

The TE and TM dual series systems can be reduced to more manageable and physically revealing forms with several manipulations. First, by introducing for $n \geqslant 1$ the functions χ_n^ϕ and χ_n^ψ so that

$$j_n(ka)h_n(ka) = (1 + \chi_n^\phi)/ika(2n+1), \tag{4.1}$$

$$[kaj_n(ka)]'[kah_n(ka)]'$$
$$= -[n(n+1)/ika(2n+1)](1 + \chi_n^\psi), \tag{4.2}$$

the dual series systems (3.7) and (3.8) can be rewritten as

$$\sum_{n=m}^{\infty} \frac{A_{mn}}{n+\frac{1}{2}} (1 + \chi_n^\phi) P_n^{-m}$$
$$= 2ika\alpha_m P_0^{-m} + 2ika \sum_{n=m}^{\infty} f_{mn} P_n^{-m} \quad (0 \leqslant \theta < \theta_0),$$

$$\sum_{n=m}^{\infty} A_{mn} P_n^{-m} = \overline{\alpha}_m \overline{P}_0^{-m} \quad (\theta_0 < \theta \leqslant \pi);$$

$$\sum_{n=m}^{\infty} B_{mn} \frac{n(n+1)}{n+\frac{1}{2}} (1 + \chi_n^\psi) P_n^{-m}$$
$$= -2ika\beta_m P_0^{-m} - 2ika$$
$$\times \sum_{n=m}^{\infty} g_{mn} P_n^{-m} \quad (0 \leqslant \theta < \theta_0),$$

$$\sum_{n=m}^{\infty} B_{mn} P_n^{-m} = \overline{\beta}_m \overline{P}_0^{-m} \quad (\theta_0 < \theta \leqslant \pi).$$

As shown in the Appendix, in the quasistatic limit

$$\lim_{ka\to 0} \chi_n^\phi = 0 + \mathscr{O}((ka)^2), \tag{4.3a}$$

$$\lim_{ka\to 0} \chi_n^\psi = 0 + \mathscr{O}((ka)^2). \tag{4.3b}$$

Thus, in analogy with the dual series treatments of the two-dimensional slit cylinder coupling problems given in Refs. 20–23, the static terms have been extracted. These TE and TM dual series must now be solved subject to Meixner's edge conditions; i.e., one must account for the singular behavior near the rim of the aperture required by the finite energy condition. The large n behavior of the solution coefficients is responsible for this edge behavior. Since, as shown in the Appendix, for large values of this index

$$\lim_{n\to\infty} \chi_n^\phi \sim \mathscr{O}(n^{-2}), \tag{4.4a}$$

$$\lim_{n\to\infty} \chi_n^\psi \sim \mathscr{O}(n^{-2}), \tag{4.4b}$$

the terms proportional to χ_n^ϕ and χ_n^ψ are of order n^{-2} smaller than the static pieces. To enhance the isolation of the large index behavior in the TM systems, we introduce the additional functions

$$\tilde{\chi}_n^\psi = n(n+1)(1+\chi_n^\psi)/(n+\tfrac{1}{2})^2 - 1$$
$$= -\{1 + [4ika/(2n+1)][kaj_n(ka)]'$$
$$\times [kah_n(ka)]'\}, \tag{4.5}$$

which exhibit the limiting behaviors

$$\lim_{n\to\infty} \tilde{\chi}_n^\psi = \mathscr{O}(n^{-2}) \text{ and } \lim_{ka\to 0} \tilde{\chi}_n^\psi = -(2n+1)^{-2}, \tag{4.6}$$

and rewrite the TM dual series systems as

$$\sum_{n=m}^{\infty} B_{mn}\left(n + \frac{1}{2}\right)(1 + \tilde{\chi}_n^\psi) P_n^{-m}$$
$$= -2ika\beta_m P_0^{-m} - 2ika$$
$$\times \sum_{n=m}^{\infty} g_{mn} P_n^{-m} \quad (0 \leqslant \theta < \theta_0), \tag{4.7}$$

$$\sum_{n=m}^{\infty} B_{mn} P_n^{-m} = \overline{\beta}_m \overline{P}_0^{-m} \quad (\theta_0 < \theta \leqslant \pi).$$

Downloaded 21 Nov 2006 to 150.135.222.53. Redistribution subject to AIP license or copyright, see http://jmp.aip.org/jmp/copyright.jsp

We then treat the terms proportional to χ_n^ϕ in (4.2) and $\tilde{\chi}_n^\psi$ in (4.7) as forcing terms by moving them to the right-hand sides. This isolates the pieces responsible for the singularities near the rim of the aperture on the left-hand sides. Defining the forcing terms

$$F_{mn} = 2ikaf_{mn} - [A_{mn}/(n+\tfrac{1}{2})]\chi_n^\phi, \tag{4.8a}$$

$$G_{mn} = -2ikag_{mn} - \tilde{\chi}_n^\psi(n+\tfrac{1}{2})B_{mn}, \tag{4.8b}$$

the TE and TM dual series systems for $m\geqslant 1$ become

$$\sum_{n=m}^\infty \frac{A_{mn}}{n+\frac{1}{2}} P_n^{-m} = 2ika\alpha_m P_0^{-m} + \sum_{n=m}^\infty F_{mn}P_n^{-m} \quad (0\leqslant\theta<\theta_0), \tag{4.9a}$$

$$\sum_{n=m}^\infty A_{mn}\overline{P}_n^{-m} = \overline{\alpha}_m \overline{P}_0^{-m} \quad (\theta_0<\theta\leqslant\pi); \tag{4.9b}$$

$$\sum_{n=m}^\infty B_{mn}\left(n+\frac{1}{2}\right)P_n^{-m} = -2ika\beta_m P_0^{-m} + \sum_{n=m}^\infty G_{mn}P_n^{-m} \quad (0\leqslant\theta<\theta_0), \tag{4.10a}$$

$$\sum_{n=m}^\infty B_{mn}\overline{P}_n^{-m} = \overline{\beta}_m \overline{P}_0^{-m} \quad (\theta_0<\theta\leqslant\pi). \tag{4.10b}$$

Equation (3.5) has been invoked to convert the P_n^{-m} to their duals $\overline{P}_n^{-m}$ over the aperture interval. This form of the dual series systems strongly suggests the solution process we introduce below.

For $m=0$, the TM dual series becomes

$$\sum_{n=1}^\infty B_{0n}\left(n+\frac{1}{2}\right)P_n = -2ika\beta_0 + \sum_{n=1}^\infty G_{0n}P_n \quad (0\leqslant\theta<\theta_0), \tag{4.10a$'$}$$

$$\sum_{n=1}^\infty B_{0n}P_n = \overline{\beta}_0 \quad (\theta_0<\theta\leqslant\pi), \tag{4.10b$'$}$$

since $P_n^0\equiv P_n$, Legendre's polynomial, and $B_{00}\equiv g_{00}\equiv 0$.

The singular behavior of the fields near the aperture rim $(\theta=\theta_0)$ is reflected in the corresponding behavior of the current components

$$\begin{aligned} J_\theta(\theta,\phi) &= H_\phi^<(a,\theta,\phi) - H_\phi^>(a,\theta,\phi) \\ &= \left[\frac{-Y_0E_0}{(ka)^2}\right]\sum_{m=0}^\infty \cos m\phi \sum_{n=m}^\infty \left\{A_{mn}\left[\frac{mP_n^{-m}(\cos\theta)}{\sin\theta}\right] + ikaB_{mn}\left[\frac{\partial}{\partial\theta}P_n^{-m}(\cos\theta)\right]\right\}, \end{aligned} \tag{4.11a}$$

$$\begin{aligned} J_\phi(\theta,\phi) &= H_\theta^>(a,\theta,\phi) - H_\theta^<(a,\theta,\phi) \\ &= \left[\frac{+Y_0E_0}{(ka)^2}\right]\sum_{m=0}^\infty \sin m\phi \sum_{n=m}^\infty \left\{A_{mn}\left[\frac{\partial}{\partial\theta}P_n^{-m}(\cos\theta)\right] + ikaB_{mn}\left[\frac{mP_n^{-m}(\cos\theta)}{\sin\theta}\right]\right\}, \end{aligned} \tag{4.11b}$$

where, for instance, $H_\phi^<(a,\theta,\phi)$ $[H_\phi^>(a,\theta,\phi)]$ is the ϕ component of the magnetic field for $r\leqslant a$ $(r\geqslant a)$ evaluated at $r=a$. Because the angular dependence of the terms depending on A_{mn} and B_{mn} in these expressions is distinct, we use it to guide our constructions of the physically correct TE and TM solutions. These solutions require several summation formulas:

$$\sum_{n=0}^\infty P_n^{-m}(\cos\theta)\partial_{\theta_0}^j \cos\left(n+\frac{1}{2}\right)\theta_0 = 0 \quad (0\leqslant\theta<\theta_0), \tag{4.12a}$$

$$\sum_{n=0}^\infty \overline{P}_n^{-m}(\cos\theta)\partial_{\theta_0}^j \sin\left(n+\frac{1}{2}\right)\theta_0 = 0 \quad (\theta_0<\theta\leqslant\pi), \tag{4.12b}$$

$$\sum_{n=0}^\infty P_n^{-m}(\cos\theta)\frac{\sin(n+\frac{1}{2})\theta_0}{n+\frac{1}{2}} = \sum_{n=0}^\infty \frac{(-1)^nP_n^{-m}(\cos\theta)}{n+\frac{1}{2}} \quad (0\leqslant\theta<\theta_0), \tag{4.12c}$$

$$\sum_{n=0}^\infty \overline{P}_n^{-m}(\cos\theta)\frac{\cos(n+\frac{1}{2})\theta_0}{n+\frac{1}{2}} = \sum_{n=0}^\infty \frac{\overline{P}_n^{-m}(\cos\theta)}{n+\frac{1}{2}} \quad (\theta_0<\theta\leqslant\pi), \tag{4.12d}$$

$$\sum_{n=0}^\infty P_n^{-m}(\cos\theta)\frac{\cos(n+\frac{1}{2})\theta_0}{(n+\frac{1}{2})^2} = (\pi-\theta_0)\sum_{n=0}^\infty (-1)^n\frac{P_n^{-m}(\cos\theta)}{n+\frac{1}{2}} \quad (0\leqslant\theta<\theta_0), \tag{4.12e}$$

which are derived from the basic expressions [see Ref. 36, Eq. (3.71)]

$$\sum_{n=0}^\infty P_n^{-m}(\cos\theta)\cos\left(n+\frac{1}{2}\right)\psi = \begin{cases} \dfrac{(-1)^m(\pi/2)^{1/2}}{\Gamma(m+\frac{1}{2})}\dfrac{[\cos\psi-\cos\theta]^{m-1/2}}{\sin^m\theta} & (0<\psi<\theta), \\ 0 & (\theta<\psi<\pi) \end{cases} \tag{4.13a}$$

(modified to our sign convention) and its dual

$$\sum_{n=0}^\infty \overline{P}_n^{-m}(\cos\theta)\sin\left(n+\frac{1}{2}\right)\psi = \begin{cases} 0 & (0<\psi<\theta), \\ \dfrac{(\pi/2)^{1/2}}{\Gamma(m+1/2)}\dfrac{[\cos\theta-\cos\psi]^{m-1/2}}{\sin^m\theta} & (\theta<\psi<\pi), \end{cases} \tag{4.13b}$$

Downloaded 21 Nov 2006 to 150.135.222.53. Redistribution subject to AIP license or copyright, see http://jmp.aip.org/jmp/copyright.jsp

and the identities (see Ref. 36, 1.19 and 1.16)

$$\sum_{n=0}^{\infty}(-1)^n\frac{\cos(n+\frac{1}{2})t}{n+\frac{1}{2}}=\frac{\pi}{2}\quad(0\leqslant t<\pi),\tag{4.14a}$$

$$\sum_{n=0}^{\infty}\frac{\sin(n+\frac{1}{2})t}{n+\frac{1}{2}}=\frac{\pi}{2}\quad(0\leqslant t<\pi).\tag{4.14b}$$

A. TE dual series solution

We would like to reduce the associated Legendre function dual series system (4.9) to one in sines and cosines. This conversion would appear to be straightforward with the representations (3.3) and (3.4) and with an interchange of the summations and integrations. However, consider Meixner's edge conditions (see Ref. 26, Sec. 9.2), which, when applied to the field generated by the TE Debye potential, imply that as the edge is approached along the surface $r=a$,

$$H^s_\phi(a,\theta,\phi)\sim\partial_r(r\Phi^s_m)|_{r=a}\sim(\theta_0-\theta)^{+1/2},$$
$$H^s_\theta(a,\theta,\phi)\sim\partial_r\partial_\theta(r\Phi^s_m)|_{r=a}\sim(\theta_0-\theta)^{-1/2}.$$

The corresponding portions of J_θ and J_ϕ near $\theta=\theta_0$ must behave, respectively, as

$$\sum_{n=m}^{\infty}A_{mn}P_n^{-m}(\cos\theta)\sim(\theta_0-\theta)^{+1/2},\tag{4.15a}$$

$$\sum_{n=m}^{\infty}A_{mn}\,\partial_\theta P_n^{-m}(\cos\theta)\sim(\theta_0-\theta)^{-1/2},\tag{4.15b}$$

where $m\geqslant 1$. Analogously, the θ dependency of Eq. (4.9a) near $\theta=\theta_0$ differs from that of (4.9b) by $(\theta_0-\theta)^{+1}$. The factor $(n+\frac{1}{2})^{-1}$ in (4.9a) is responsible for this difference. Thus, with [see Ref. 37, (8.10.7) and (6.1.37)]

$$\lim_{n\to\infty}P_n^{-m}(\cos\theta)\sim n^{-m+1/2}\times\frac{\cos[(n+\frac{1}{2})\theta-m\pi/2-\pi/4]}{(\pi\sin\theta/2)^{1/2}}$$

and (4.13), Meixner's conditions are satisfied if

$$\lim_{n\to\infty}A_{mn}\sim n^{m-1}.\tag{4.16}$$

The simple summation–integration interchange is then not directly permitted because it will introduce terms that are proportional to delta functions and their derivatives; i.e., with (1.135) from Ref. 36 one finds, for instance, that near $\theta=\theta_0$

$$\sum_{n=0}^{\infty}n^j\cos\left(n+\frac{1}{2}\right)\theta\cos\left(n+\frac{1}{2}\right)\theta_0\sim\delta^{(j)}(\theta_0-\theta),$$

the jth derivative of the Dirac distribution. Interchange can be accomplished by preconditioning the dual series as follows.

We need to introduce terms into (4.9) that will cancel the potential delta function contributions. This is accomplished with Eqs. (4.12)–(4.14). In particular, we define the modified solution coefficients

$$\widetilde{A}_{mn}=\sum_{j=0}^{m-1}a_{mj}\,\partial^j_{\theta_0}\sin\left(n+\frac{1}{2}\right)\theta_0+\begin{cases}A_{mn}&(n\geqslant m\geqslant 1),\\0&(0\leqslant n<m),\end{cases}\tag{4.17}$$

and the modified forcing term coefficients

$$\widetilde{F}_{mn}=F_{mn}\quad(n\geqslant m=1),\tag{4.18a}$$

$$\widetilde{F}_{mn}=\frac{-(ka)^2}{2}\sum_{j=0}^{m-2}a_{m(j+1)}\,\partial^j_{\theta_0}\frac{\cos(n+\frac{1}{2})\theta_0}{(n+\frac{1}{2})^2}+\begin{cases}F_{mn}&(n\geqslant m\geqslant 2),\\0&(0\leqslant n<m),\end{cases}\tag{4.18b}$$

so that the TE dual series systems for $m\geqslant 1$ become

$$\sum_{n=0}^{\infty}\frac{\widetilde{A}_{mn}}{n+\frac{1}{2}}P_n^{-m}=2ika\alpha_mP_0^{-m}+(a_{m0}-\kappa^E_m)\sum_{n=0}^{\infty}\frac{(-1)^nP_n^{-m}}{n+\frac{1}{2}}+\sum_{n=0}^{\infty}\widetilde{F}_{mn}P_n^{-m}\quad(0\leqslant\theta<\theta_0),\tag{4.19a}$$

$$\sum_{n=0}^{\infty}\widetilde{A}_{mn}\overline{P}_n^{-m}=\overline{\alpha}_m\overline{P}_0^{-m}\quad(\theta_0<\theta\leqslant\pi).\tag{4.19b}$$

The constants

$$\kappa^E_m=\frac{-(ka)^2}{2}\begin{cases}0,&\text{for } m=1,\\(\pi-\theta_0)a_{m1},&\text{for } m=2,\\(\pi-\theta_0)a_{m1}-a_{m2},&\text{for } m\geqslant 3.\end{cases}\tag{4.20}$$

The additional unknown coefficients a_{mj} $(j=0,1,\ldots,m-1)$ provide the extra degrees of freedom needed to remove the unphysical singularities and permit the desired summation–integration interchange. In particular, their values will be fixed by our solution process so that for any $m\geqslant 1$

$$\lim_{n\to\infty}\widetilde{A}_{mn}\sim\mathscr{O}(n^{-1}),\tag{4.17'}$$

$$\lim_{n\to\infty}\widetilde{F}_{mn}\sim\mathscr{O}(n^{-3}).\tag{4.18'}$$

Note that it can be inferred from the form of (4.19) that we have completed the basis function set for this open geometry by including the associated Legendre polynomials P_n^{-m} and $\overline{P}_n^{-m}$ for $0\leqslant n<m$.

Inserting (3.3) and (3.4) into (4.19) and interchanging the summations and integrations, the desired TE dual series are generated:

$$\sum_{n=0}^{\infty}\frac{\widetilde{A}_{mn}}{n+\frac{1}{2}}\cos\left(n+\frac{1}{2}\right)t=\frac{\pi}{2}(a_{m0}-\kappa^E_m)+2ika\alpha_m\cos\frac{t}{2}+\sum_{n=0}^{\infty}\widetilde{F}_{mn}\cos\left(n+\frac{1}{2}\right)t\quad(0\leqslant t<\theta_0),\tag{4.21a}$$

$$\sum_{n=0}^{\infty}\widetilde{A}_{mn}\sin\left(n+\frac{1}{2}\right)t=\bar{\alpha}_m\sin\frac{t}{2}\quad(\theta_0<t\leqslant\pi).\tag{4.21b}$$

A solution of (4.21) is constructed as in Refs. 20–24 by first making the metal and aperture equations display the same t dependence. Two possibilities exist: integrating (4.21b) or differentiating (4.21a). Only the former guarantees satisfaction of (4.17′). Applying $\int_t^\pi dt$ to (4.21b) leads to the dual series system

Downloaded 21 Nov 2006 to 150.135.222.53. Redistribution subject to AIP license or copyright, see http://jmp.aip.org/jmp/copyright.jsp

$$\sum_{n=0}^{\infty} \frac{\widetilde{A}_{mn}}{n+\frac{1}{2}} \cos\left(n+\frac{1}{2}\right) t = \begin{cases} \frac{\pi}{2}(a_{m0} - \kappa_m^E) + 2ika\alpha_m \cos\frac{t}{2} + \sum_{n=0}^{\infty} \widetilde{F}_{mn} \cos\left(n+\frac{1}{2}\right) t & (0 \leqslant t < \theta_0), \\ 2\bar{\alpha}_m \cos\frac{t}{2} & (\theta_0 < t \leqslant \pi). \end{cases} \tag{4.22}$$

Since the left-hand side of (4.22) is now defined over the entire $[0,\pi]$ interval, Fourier inversion then yields the coefficients

$$\frac{\widetilde{A}_{ml}}{l+\frac{1}{2}} = (a_{m0} - \kappa_m^E) \frac{\sin(l+\frac{1}{2})\theta_0}{l+\frac{1}{2}} + (2ika\alpha_m - 2\bar{\alpha}_m)\Lambda_{0l}^E + 2\bar{\alpha}_m \delta_{0l} + \sum_{n=0}^{\infty} \widetilde{F}_{mn} \Lambda_{nl}^E \quad (l = 0,1,\ldots), \tag{4.23}$$

where the inversion terms

$$\Lambda_{nl}^E = \frac{2}{\pi} \int_0^{\theta_0} \cos\left[\left(n+\frac{1}{2}\right)\psi\right] \cos\left[\left(l+\frac{1}{2}\right)\psi\right] d\psi = \begin{cases} \frac{1}{\pi}\left[\frac{\sin(n-l)\theta_0}{n-l} + \frac{\sin(n+l+1)\theta_0}{n+l+1}\right] & (n \neq l), \\ \frac{1}{\pi}\left[\theta_0 + \frac{\sin(2l+1)\theta_0}{2l+1}\right] & (n = l). \end{cases} \tag{4.24}$$

Explicitly, (4.23) means

$$\sum_{j=1}^{m-1} a_{mj}\, \partial_{\theta_0}^j \frac{\sin(l+\frac{1}{2})\theta_0}{l+\frac{1}{2}} = (2ika\alpha_m - 2\bar{\alpha}_m)\Lambda_{0l}^E + 2\bar{\alpha}_m\delta_{0l} - \kappa_m^E \frac{\sin(l+\frac{1}{2})\theta_0}{l+\frac{1}{2}} + \sum_{n=0}^{\infty} \widetilde{F}_{mn}\Lambda_{nl}^E \quad (l = 0,1,\ldots,m-1), \tag{4.23'}$$

$$\frac{A_{ml}}{l+\frac{1}{2}} = -\sum_{j=1}^{m-1} a_{mj}\, \partial_{\theta_0}^j \frac{\sin(l+\frac{1}{2})\theta_0}{l+\frac{1}{2}} + (2ika\alpha_m - 2\bar{\alpha}_m)\Lambda_{0l}^E + 2\bar{\alpha}_m\delta_{0l} - \kappa_m^E \frac{\sin(l+\frac{1}{2})\theta_0}{l+\frac{1}{2}} + \sum_{n=0}^{\infty} \widetilde{F}_{mn}\Lambda_{nl}^E \quad (l = m,m+1,\ldots). \tag{4.23''}$$

Furthermore, inversion requires continuity of the right-hand side of (4.22) across $t = \theta_0$. This yields

$$a_{m0} = \kappa_m^E - \frac{2}{\pi}\left[(2ika\alpha_m - 2\bar{\alpha}_m)\cos\frac{\theta_0}{2} + \sum_{n=0}^{\infty} \widetilde{F}_{mn} \cos\left(n+\frac{1}{2}\right)\theta_0\right]. \tag{4.25}$$

The system (4.23) and (4.25) is an infinite system of linear equations for the TE solution coefficients. The first $(m+1)$ of these, (4.23') and Eq. (4.25), would not have appeared without the introduction of the terms a_{mj}, α_n, and $\bar{\alpha}_n$; hence, the terms $\cos(n+\frac{1}{2})\theta$ and $\sin(n+\frac{1}{2})\theta$ for $n = 0,1,\ldots,m-1$ into (4.21). The Λ_{0l}^E $(l = 0,1,\ldots)$ terms originate in this completion of the expansion. Moreover, since there are no solution coefficients A_{mn} $(0 \leqslant n < m)$ in those first $(m+1)$ equations, we may view them as orthogonality relations. They determine the interchange coefficients a_{mj} $(j = 1,\ldots,m-1)$ and a relation between the decoupling coefficients α_m and $\bar{\alpha}_m$. In a similar fashion, the TM case generates a relation between β_m and $\bar{\beta}_m$. The remaining two degrees of freedom are determined by the constraint relations (3.10) and (3.11). The coefficient a_{m0} is defined by (4.25) and is coupled to all of the other a_{mj} $(j = 1,\ldots,m-1)$ through the relation for $(2ika\alpha_m - 2\bar{\alpha}_m)$. However, it does not contribute directly to the solution coefficients A_{ml} $(l = m,m+1,\ldots)$. It only provides that degree of freedom needed to insure continuity across the boundary between the metal and aperture intervals.

Equations (4.23) are solutions of the original dual series (4.9) subject to Meixner's edge conditions (4.15a). They are general solutions if these results are independent of the decoupling and interchange constants. This has been confirmed numerically for $m = 1,2,3$. A rich set of new associated Legendre polynomial identities is obtained from this validation process.[25] We consider explicitly only the $m = 1$ relations since they are employed for the normal incidence case discussed below.

For $m = 1$, the solution system

$$\frac{A_{1l}}{l+\frac{1}{2}} = (2ika\alpha_1 - 2\bar{\alpha}_1)\Lambda_{0l}^E + \sum_{n=1}^{\infty} F_{1n}\Lambda_{nl}^E \quad (l = 1,2,\ldots), \tag{4.26a}$$

$$0 = (2ika\alpha_1 - 2\bar{\alpha}_1)\Lambda_{00}^E + 2\bar{\alpha}_1 + \sum_{n=1}^{\infty} F_{1n}\Lambda_{n0}^E, \tag{4.26b}$$

gives the coefficients

$$\frac{A_{1l}}{l+\frac{1}{2}} = \sum_{n=1}^{\infty} F_{1n}\Gamma_{1,nl}^E + 2\bar{\alpha}_1 L_{1l}^E \quad (l = 1,2,\ldots), \tag{4.27a}$$

where

$$\Gamma_{1,nl}^E = \Lambda_{nl}^E - \Lambda_{n0}^E\Lambda_{0l}^E/\Lambda_{00}^E, \tag{4.27b}$$

$$L_{1l}^E = -\Lambda_{0l}^E/\Lambda_{00}^E. \tag{4.27c}$$

Substituting these expressions into the $m = 1$ versions of (4.9a) and (4.9b), the original dual series system is satisfied since *on the metal* $(0 \leqslant \theta < \theta_0)$

$$\sum_{l=1}^{\infty} \Gamma_{1,nl}^E P_l^{-1} - P_n^{-1} - L_{1n}^E P_0^{-1} = 0 \quad (n = 1,2,\ldots), \tag{4.28a}$$

$$\sum_{l=1}^{\infty} L_{1l}^E P_l^{-1} - \frac{\Lambda_{00}^E - 1}{\Lambda_{00}^E} P_0^{-1} = 0, \tag{4.28b}$$

and *in the aperture* $(\theta_0 < \theta \leqslant \pi)$

$$\sum_{l=1}^{\infty} (2l+1)\Gamma_{nl}^E P_l^{-1} = 0 \quad (n = 1,2,\ldots), \tag{4.29a}$$

$$\sum_{l=1}^{\infty} (2l+1) L_{1l}^E - \bar{P}_0^{-1} = 0. \tag{4.29b}$$

Downloaded 21 Nov 2006 to 150.135.222.53. Redistribution subject to AIP license or copyright, see http://jmp.aip.org/jmp/copyright.jsp

When evaluated over the metal interval ($0 \leqslant \theta < \theta_0$), the left-hand sides of Eqs. (4.29) yield Eqs. (4.15).

B. TM dual series solution

We proceed as in the TE case. Consider the dual series systems (4.10) and (4.10'). Meixner's edge conditions applied to the fields generated by the TM Debye potential imply that near $\theta = \theta_0$

$$H^s_\theta(a,\theta,\phi) \sim (r\Psi^s_m)|_{r=a} \sim (\theta_0 - \theta)^{+3/2},$$
$$H^s_\phi(a,\theta,\phi) \sim \partial_\theta(r\Psi^s_m)|_{r=a} \sim (\theta_0 - \theta)^{+1/2}.$$

Thus, from (4.11a) and (4.11b), the portions of J_θ and J_ϕ generated by Ψ^s_m near the aperture edge behave, respectively, as

$$\sum_{n=m}^{\infty} B_{mn} P_n^{-m}(\cos\theta) \sim (\theta_0 - \theta)^{+3/2}, \tag{4.30a}$$

$$\sum_{n=m}^{\infty} B_{mn}\, \partial_\theta P_n^{-m}(\cos\theta) \sim (\theta_0 - \theta)^{+1/2}, \tag{4.30b}$$

where $m \geqslant 0$. Analogously, the θ dependency of the metal equations near $\theta = \theta_0$ differs from that of the aperture equations by $(\theta_0 - \theta)^{-1}$. The factor $(n + \frac{1}{2})$ in the metal equations is responsible for this difference.

The requisite edge behavior (4.30a) is obtained if

$$\lim_{n\to\infty} B_{mn} \sim n^{m-2}. \tag{4.31}$$

Consider first the cases with $m > 0$. Anticipating the effects of the operator interchange, we introduce the modified coefficients

$$\widetilde{B}_{mn} = \sum_{j=0}^{m-1} b_{mj}\, \partial^j_{\theta_0} \frac{\cos(n+\frac{1}{2})\theta_0}{n+\frac{1}{2}} + \begin{cases} B_{mn} & (n \geqslant m \geqslant 1), \\ 0 & (0 \leqslant n < m), \end{cases} \tag{4.32}$$

the modified forcing term coefficients

$$\widetilde{G}_{mn} = G_{mn} \quad (n \geqslant m = 1), \tag{4.33a}$$

$$\widetilde{G}_{mn} = \frac{(ka)^2}{2} \sum_{j=0}^{m-2} b_{m(j+1)}\, \partial^j_{\theta_0} \frac{\sin(n+\frac{1}{2})\theta_0}{n+\frac{1}{2}} + \begin{cases} G_{mn} & (n \geqslant m \geqslant 2), \\ 0 & (0 \leqslant n < m), \end{cases} \tag{4.33b}$$

and the constants

$$\kappa^H_m = \begin{cases} 0, & \text{for } m = 1, \\ [(ka)^2/2] b_{m1}, & \text{for } m \geqslant 2. \end{cases} \tag{4.33c}$$

The interchange constants b_{mj} ($j = 0,1,\ldots,m-1$) will be adjusted so that for all $m \geqslant 1$

$$\lim_{n\to\infty} \widetilde{B}_{mn} \sim \mathscr{O}(n^{-2}), \tag{4.32'}$$

$$\lim_{n\to\infty} \widetilde{G}_{mn} \sim \mathscr{O}(n^{-3}). \tag{4.33'}$$

The dual series systems (4.10) become

$$\sum_{n=0}^{\infty} \left(n + \frac{1}{2}\right) \widetilde{B}_{mn} P_n^{-m} = -2ika\beta_m P_0^{-m} + \sum_{n=0}^{\infty} \widetilde{G}_{mn} P_n^{-m} - \kappa^H_m \times \sum_{n=0}^{\infty} \frac{(-1)^n P_n^{-m}}{n+\frac{1}{2}} \quad (0 \leqslant \theta < \theta_0), \tag{4.34a}$$

$$\sum_{n=0}^{\infty} \widetilde{B}_{mn} \bar{P}_n^{-m} = \bar{\beta}_m \bar{P}_0^{-m} + b_{m0} \sum_{n=0}^{\infty} \frac{\bar{P}_n^{-m}}{n+\frac{1}{2}} \quad (\theta_0 < \theta \leqslant \pi). \tag{4.34b}$$

Introducing (3.3) and (3.4), interchanging summations and integrations, and applying the operator $\int_0^t dt$ to the resulting metal equation to attain similar t dependencies for both equations, the TM dual series prior to inversion are

$$\sum_{n=0}^{\infty} \widetilde{B}_{mn} \sin\left(n+\frac{1}{2}\right)t = \begin{cases} -4ika\beta_m \sin\dfrac{t}{2} + \displaystyle\sum_{n=0}^{\infty} \frac{\widetilde{G}_{mn}}{n+\frac{1}{2}} \sin\left(n+\frac{1}{2}\right)t - \kappa^H_m \frac{\pi}{2} t & (0 \leqslant t < \theta_0), \\ \bar{\beta}_m \sin\dfrac{t}{2} + b_{m0} \dfrac{\pi}{2} & (\theta_0 < t \leqslant \pi). \end{cases} \tag{4.35}$$

Introducing the terms

$$\mu_l(\theta_0) = \int_0^{\theta_0} t \sin\left(l+\frac{1}{2}\right)t = \frac{\sin(l+\frac{1}{2})\theta_0}{(l+\frac{1}{2})^2} - \theta_0 \frac{\cos(l+\frac{1}{2})\theta_0}{l+\frac{1}{2}}, \tag{4.36}$$

$$\Lambda^H_{nl} = \frac{2}{\pi} \int_0^{\theta_0} \sin\left[\left(n+\frac{1}{2}\right)\psi\right] \sin\left[\left(l+\frac{1}{2}\right)\psi\right] d\psi = \begin{cases} \dfrac{1}{\pi}\left[\dfrac{\sin(n-l)\theta_0}{n-l} - \dfrac{\sin(n+l+1)\theta_0}{n+l+1}\right] & (n \neq l), \\ \dfrac{1}{\pi}\left[\theta_0 - \dfrac{\sin(2l+1)\theta_0}{2l+1}\right] & (n = l), \end{cases} \tag{4.37}$$

Fourier inversion leads to the coefficient expressions for $m \geqslant 1$

$$\widetilde{B}_{ml} = -(4ika\beta_m + \bar{\beta}_m)\Lambda^H_{0l} + \bar{\beta}_m \delta_{0l} + b_{m0} \frac{\cos(l+\frac{1}{2})\theta_0}{l+\frac{1}{2}} - \kappa^H_m \mu_l(\theta_0) + \sum_{n=0}^{\infty} \frac{\widetilde{G}_{mn}}{n+\frac{1}{2}} \Lambda^H_{nl} \quad (l = 0,1,\ldots). \tag{4.38a}$$

These contain explicitly m orthogonality relations

$$\sum_{j=0}^{m-1} b_{mj}\, \partial^j_{\theta_0} \frac{\cos(l+\frac{1}{2})\theta_0}{l+\frac{1}{2}} = -(4ika\beta_m + \bar{\beta}_m)\Lambda^H_{0l} + \bar{\beta}_m \delta_{0l} + b_{m0} \frac{\cos(l+\frac{1}{2})\theta_0}{l+\frac{1}{2}} - \kappa^H_m \mu_l(\theta_0) + \sum_{n=0}^{\infty} \frac{\widetilde{G}_{mn}}{n+\frac{1}{2}} \Lambda^H_{nl}$$
$$(l = 0,\ldots,m-1), \tag{4.38b}$$

Downloaded 21 Nov 2006 to 150.135.222.53. Redistribution subject to AIP license or copyright, see http://jmp.aip.org/jmp/copyright.jsp

and the coefficients

$$B_{ml} = -(4ika\beta_m + \bar{\beta}_m)\Lambda_{0l}^H + \bar{\beta}_m\delta_{0l} - \kappa_m^H\mu_l(\theta_0) - \sum_{j=1}^{m-1} b_{mj}\,\partial_{\theta_0}^j \frac{\cos(l+\frac{1}{2})\theta_0}{l+\frac{1}{2}} + \sum_{n=0}^{\infty} \frac{\tilde{G}_{mn}}{n+\frac{1}{2}}\Lambda_{nl}^H$$
$$(l = m, m+1, \ldots). \quad (4.38c)$$

Continuity across $t = \theta_0$ of the right-hand side of (4.35) gives

$$b_{m0} = -\kappa_m^H\theta_0 - \frac{2}{\pi}\left[(4ika\beta_m + \bar{\beta}_m)\sin\frac{\theta_0}{2} - \sum_{n=0}^{\infty}\frac{\tilde{G}_{mn}}{n+\frac{1}{2}}\sin\left(n+\frac{1}{2}\right)\theta_0\right]. \quad (4.39)$$

Note that b_{m0} does not contribute directly to the solution coefficients B_{ml} $(l = m, m+1, \ldots)$.

Equations (4.38) are general solutions of (4.10) subject to Meixner's edge conditions (4.30b). As with the TE case, this has been confirmed numerically for $m = 1,2,3$. Explicitly for $m = 1$ the resulting solution system

$$B_{1l} = -(4ika\beta_1 + \bar{\beta}_1)\Lambda_{0l}^H + \sum_{n=1}^{\infty}\frac{G_{1n}}{n+\frac{1}{2}}\Lambda_{nl}^H$$
$$(l = 1,2,\ldots), \quad (4.40a)$$

$$0 = \bar{\beta}_1 - (4ika\beta_1 + \bar{\beta}_1)\Lambda_{00}^H + \sum_{n=1}^{\infty}\frac{G_{1n}}{n+\frac{1}{2}}\Lambda_{n0}^H \quad (4.40b)$$

yields the coefficients

$$B_{1l} = \sum_{n=1}^{\infty}\frac{G_{1n}}{n+\frac{1}{2}}\Gamma_{1,nl}^H + \bar{\beta}_1 L_{1l}^H \quad (l = 1,2,\ldots), \quad (4.41a)$$

where

$$\Gamma_{1,nl}^H = \Lambda_{nl}^H - \Lambda_{n0}^H\Lambda_{0l}^H/\Lambda_{00}^H, \quad (4.41b)$$

$$L_{1l}^H = -\Lambda_{0l}^H/\Lambda_{00}^H. \quad (4.41c)$$

Satisfaction of the $m = 1$ versions of the original dual series system (4.10) is guaranteed since *on the metal* $(0 \leqslant \theta < \theta_0)$,

$$\sum_{l=1}^{\infty}(2l+1)\Gamma_{1,nl}^H P_l^{-1} - (2n+1)P_n^{-1} - L_{1n}^H P_0^{-1} = 0 \quad (n = 1,2,\ldots), \quad (4.42a)$$

$$\sum_{l=1}^{\infty}(2l+1)L_{1l}^H P_l^{-1} - \frac{\Lambda_{00}^H - 1}{\Lambda_{00}^H}P_0^{-1} = 0, \quad (4.42b)$$

and since *in the aperture* $(\theta_0 < \theta \leqslant \pi)$,

$$\sum_{l=1}^{\infty}\Gamma_{1,nl}^H P_l^{-1} = 0, \quad (4.43a)$$

$$\sum_{l=1}^{\infty}L_{1l}^H P_l^{-1} - \bar{P}_0^{-1} = 0. \quad (4.43b)$$

Finally, consider the $m = 0$ case. Introducing the modified coefficients

$$\tilde{B}_{0n} = \begin{cases} B_{00} & (n = 0), \\ B_{0n} & (n \geqslant 1), \end{cases} \quad (4.44)$$

and the modified constants

$$\beta_0' = \beta_0 - B_{00}/4ika, \quad (4.45a)$$

$$\bar{\beta}_0' = \bar{\beta}_0 + B_{00}, \quad (4.45b)$$

the dual series system (4.8′) can be rewritten as

$$\sum_{n=0}^{\infty}\left(n+\frac{1}{2}\right)\tilde{B}_{0n}P_n = -2ika\beta_0' P_0 + \sum_{n=1}^{\infty}G_{0n}P_n$$
$$(0 \leqslant \theta < \theta_0), \quad (4.46a)$$

$$\sum_{n=0}^{\infty}\tilde{B}_{0n}P_n = \bar{\beta}_0' P_0 \quad (\theta_0 < \theta \leqslant \pi). \quad (4.46b)$$

Our TM solution process leads to the solution coefficients

$$B_{0l} = \sum_{n=1}^{\infty}\frac{G_{0n}}{n+\frac{1}{2}}\Gamma_{0,nl}^H \quad (l = 1,2,\ldots), \quad (4.47a)$$

where

$$\Gamma_{0,nl}^H = \Lambda_{nl}^H - \frac{\sin(n+\frac{1}{2})\theta_0}{\sin\theta_0/2}\Lambda_{0l}^H \quad (4.47b)$$

and the constant

$$\bar{\beta}_0 = -\sum_{n=1}^{\infty}\frac{G_{0n}}{n+\frac{1}{2}}\Gamma_{0,n0}^H. \quad (4.47c)$$

The remaining constant β_0 follows immediately from the continuity condition:

$$(4ika\beta_0' + \bar{\beta}_0') \equiv 4ika\beta_0 + \bar{\beta}_0 = \sum_{n=1}^{\infty}\frac{G_{0n}}{n+\frac{1}{2}}\frac{\sin(n+\frac{1}{2})\theta_0}{\sin\theta_0/2}. \quad (4.48)$$

C. Coupled TE and TM solution systems

The modal coefficients of the original electromagnetics problem can now be constructed from the TE and TM dual series results. The TE solution systems for $m \geqslant 1$, (4.23), are still coupled to the corresponding TM solution systems (4.38) through the constraint relations (3.10) and (3.11). For $m = 0$ only TM coefficients exist, and they are generated from (4.47). For each m an infinite linear system of the form (an invertible Fredholm system of the second kind)

$$V_{ml} + \sum_{n=0}^{\infty}\mathscr{M}_{m,nl}V_{mn} = \sum_{n=0}^{\infty}\mathscr{N}_{m,nl}W_{mn} \quad (l = 0,1,2,\ldots) \quad (4.49)$$

is obtained and must be solved. A solution process analogous to the one developed in Ref. 20 can then be applied.

The infinite linear system (4.49) is reduced to a finite one by recognizing that as $n \to \infty$ several terms rapidly go to zero. In particular, the TE and TM solutions have been constructed so that for all m

$$\lim_{n\to\infty}\mathscr{M}_{m,nl} \sim \mathscr{O}(n^{-3}), \quad (4.50a)$$

$$\lim_{n\to\infty}W_{mn} \sim \mathscr{O}(n^{m-3/2-n}). \quad (4.50b)$$

Let us assume that N unknown coefficients are desired: $V_{m1},\ldots,V_{mN}$. Truncation then occurs in (4.49) after the Nth term and the following square system results:

$$V_{ml} + \sum_{n=0}^{N}\mathscr{M}_{m,nl}V_{mn} = \sum_{n=0}^{N}\mathscr{N}_{m,nl}W_{mn} \quad (l = 0,1,\ldots,N). \quad (4.51)$$

This system can be solved numerically, for instance, by Gauss elimination. Any additional coefficients can then be

Downloaded 21 Nov 2006 to 150.135.222.53. Redistribution subject to AIP license or copyright, see http://jmp.aip.org/jmp/copyright.jsp

generated recursively from (4.51) by setting $l = N+1, N+2,\ldots,L$.

To illustrate this procedure, consider the $m=1$ case. Introducing the terms $\xi = -\bar{\beta}_1$, $\eta = \alpha_1$, $\bar{f}_{1n} = 2ikaf_{1n}$, $\bar{g}_{1n} = -2ikag_{1n}/(n+\frac{1}{2})$, and $\bar{A}_{1n} = A_{1n}/(n+\frac{1}{2})$ and combining the constraint conditions (3.10) and (3.11), the orthogonality relations (4.26b) and (4.40b), and the coefficient expressions (4.27) and (4.41), one obtains the solution system ($l = 1,2,\ldots$)

$$(2ikaL^E_{1l})\xi + \bar{A}_{1l} + \sum_{n=1}^{\infty} (\chi^\phi_n \Gamma^E_{1,nl})\bar{A}_{1n} = \sum_{n=1}^{\infty} \Gamma^E_{1,nl}\bar{f}_{1n}, \tag{4.52a}$$

$$(L^H_{1l})\xi + B_{1l} + \sum_{n=1}^{\infty} (\tilde{\chi}^\psi_n \Gamma^H_{1,nl})B_{1n} = \sum_{n=1}^{\infty} \Gamma^H_{1,nl}\bar{g}_{1n}, \tag{4.52b}$$

$$[2ika(1-\Lambda^E_{00})]\xi + (-2ika\Lambda^E_{00})\eta + \sum_{n=1}^{\infty} (\chi^\phi_n \Lambda^E_{n0})\bar{A}_{1n} = \sum_{n=1}^{\infty} \Lambda^E_{n0}\bar{f}_{1n}, \tag{4.52c}$$

$$(1-\Lambda^H_{00})\xi + [-4(ka)^2\Lambda^H_{00}]\eta + \sum_{n=1}^{\infty} (\tilde{\chi}^\psi_n \Lambda^H_{n0})B_{1n} = \sum_{n=1}^{\infty} \Lambda^H_{n0}\bar{g}_{1n}. \tag{4.52d}$$

These equations clearly are coupled and take the form of (4.49). The infinite system (4.52) is reduced to a finite one by noticing that

$$\lim_{n\to\infty} \chi^\phi_n \Gamma^E_{1,nl} \sim \lim_{n\to\infty} \chi^\psi_n \Gamma^H_{1,nl} \sim \mathscr{O}(n^{-3}), \tag{4.53a}$$

$$\lim_{n\to\infty} \bar{f}_{1n} \sim \lim_{n\to\infty} \bar{g}_{1n} \sim \mathscr{O}(n^{-(n+1/2)}). \tag{4.53b}$$

Assuming that the coefficients $\bar{A}_{1n}$ and B_{1n} are desired for $n = 1,\ldots,N$, the truncated solution system is

$$(2ikaL^E_{1l})\xi + \bar{A}_{1l} + \sum_{n=1}^{N} (\chi^\phi_n \Gamma^E_{1,nl})\bar{A}_{1n} = \sum_{n=1}^{N} \Gamma^E_{1,nl}\bar{f}_{1n} \quad (l = 1,2,\ldots,N), \tag{4.54a}$$

$$(L^E_{1l})\xi + B_{1l} + \sum_{n=1}^{N} (\tilde{\chi}^\psi_n \Gamma^H_{1,nl})B_{1n} = \sum_{n=1}^{N} \Gamma^E_{1,nl}\bar{g}_{1n} \quad (l = 1,2,\ldots,N), \tag{4.54b}$$

$$[2ika(1-\Lambda^E_{00})]\xi + (-2ika\Lambda^E_{00})\eta + \sum_{n=1}^{N} (\chi^\phi_n \Lambda^E_{n0})\bar{A}_{1n} = \sum_{n=1}^{N} \Lambda^E_{n0}\bar{f}_{1n}, \tag{4.54c}$$

$$(1-\Lambda^H_{00})\xi + [-4(ka)^2\Lambda^H_{00}]\eta + \sum_{n=1}^{N} (\tilde{\chi}^\psi_n \Lambda^H_{n0})B_{1n} = \sum_{n=1}^{\infty} \Lambda^H_{n0}\bar{g}_{1n}. \tag{4.54d}$$

Numerical results generated from this system will be presented below.

V. NORMAL INCIDENCE CASE

The plane wave is normally incident when $\theta^{\text{inc}} = 0$ or $\theta^{\text{inc}} = \pi$. The $\theta^{\text{inc}} = 0$ geometry is illustrated in Fig. 2. The

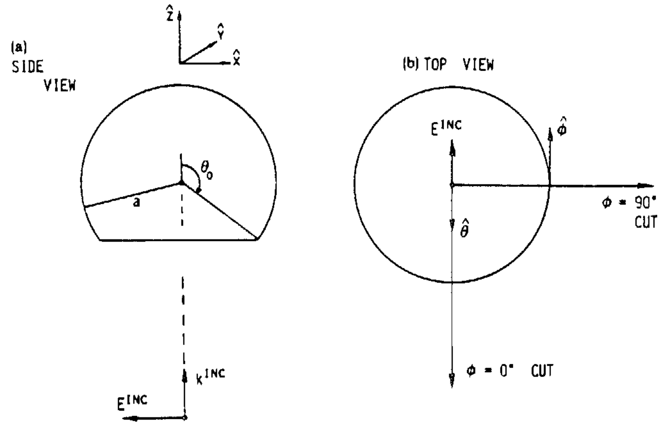

FIG. 2. Configuration of the scattering of a normally incident plane wave from a spherical shell having a circular aperture: (a) side view, (b) top view.

restriction to normal incidence provides a great simplification because

$$\left[\frac{mP^m_n(\cos\theta)}{\sin\theta}\right](\theta = \theta^{\text{inc}} = 0) = \left[+\frac{\partial}{\partial\theta}P^m_n(\cos\theta)\right](\theta = \theta^{\text{inc}} = 0) = \frac{n(n+1)}{2}\delta_{m1}, \tag{5.1}$$

$$\left[\frac{mP^m_n(\cos\theta)}{\sin\theta}\right](\theta = \theta^{\text{inc}} = \pi) = \left[-\frac{\partial}{\partial\theta}P^m_n(\cos\theta)\right](\theta = \theta^{\text{inc}} = \pi) = (-1)^{n+1}\frac{n(n+1)}{2}\delta_{m1}. \tag{5.2}$$

As a result, the potentials reduce to single sums involving only the $m=1$ azimuthal mode:

$$\begin{pmatrix}\Phi^{\text{inc}}\\ \Phi^s\end{pmatrix} = -E_0\begin{pmatrix}\Phi^{\text{inc}}_1\\ \Phi^s_1\end{pmatrix}\sin\phi, \tag{5.3a}$$

$$\begin{pmatrix}\Psi^{\text{inc}}\\ \Psi^s\end{pmatrix} = Y_0E_0\begin{pmatrix}\Psi^{\text{inc}}_1\\ \Psi^s_1\end{pmatrix}\cos\phi. \tag{5.3b}$$

Consequently, the coupled dual series systems for normal incidence coincide with the $m=1$ case treated in Sec. IV; the modal coefficients A_{1n} and B_{1n} are numerically generated from the solution system (4.54) with $\theta^{\text{inc}} = 0$ or π. The field components for normal incidence in terms of these coefficients are listed in Table II for convenient reference. These expressions isolate the coefficients, the r, the θ, and the ϕ dependencies; hence they are very useful for current, energy density, and cross section calculations.

An important analytical property of the dual series solution is simply revealed by the normal incidence case results. This is its trivial recovery of the scattering coefficients for the closed sphere case when $\theta_0 = \pi$. Let $\theta^{\text{inc}} = 0$. The terms

$$\Lambda^{E,H}_{nl}(\theta_0 = \pi) = \delta_{nl}, \tag{5.4}$$

Downloaded 21 Nov 2006 to 150.135.222.53. Redistribution subject to AIP license or copyright, see http://jmp.aip.org/jmp/copyright.jsp

TABLE II. Electric and magnetic field components for normal incidence.

Field components

$$E_r = E_0 \sum_{n=1}^{\infty} in(n+1)\tau_{1n} \frac{Z_n(kr)}{kr} P_n^{-1}(\cos\theta)\cos\phi$$

$$E_\theta = E_0 \sum_{n=1}^{\infty} \left\{\sigma_{1n} Z_n(kr)\bar{v}_{1n}(\theta) - i\tau_{1n} \frac{[krZ_n(kr)]'}{kr} \bar{w}_{1n}(\theta)\right\}\cos\phi$$

$$E_\phi = E_0 \sum_{n=1}^{\infty} \left\{\sigma_{1n} Z_n(kr)\bar{w}_{1n}(\theta) - i\tau_{1n} \frac{[krZ_n(kr)]'}{kr} \bar{v}_{1n}(\theta)\right\}\sin\phi$$

$$H_r = -Y_0E_0 \sum_{n=1}^{\infty} in(n+1)\sigma_{1n} \frac{Z_n(kr)}{kr} P_n^{-1}(\cos\theta)\sin\phi$$

$$H_\theta = -Y_0E_0 \sum_{n=1}^{\infty} \left\{\tau_{1n} Z_n(kr)\bar{v}_{1n}(\theta) - i\sigma_{1n} \frac{[krZ_n(kr)]'}{kr} \bar{w}_{1n}(\theta)\right\}\sin\phi$$

$$H_\phi = +Y_0E_0 \sum_{n=1}^{\infty} \left\{\tau_{1n} Z_n(kr)\bar{w}_{1n}(\theta) - i\sigma_{1n} \frac{[krZ_n(kr)]'}{kr} \bar{v}_{1n}(\theta)\right\}\cos\phi$$

Incident field

$Z_n(kr) = j_n(kr)$

$$\sigma_{1n}^{\text{inc}} = i^n(2n+1)\begin{cases} 1, & \theta^{\text{inc}} = 0 \\ (-1)^{n+1}, & \theta^{\text{inc}} = \pi \end{cases}$$

$$\tau_{1n}^{\text{inc}} = i^n(2n+1)\begin{cases} -1, & \theta^{\text{inc}} = 0 \\ (-1)^{n+1}, & \theta^{\text{inc}} = \pi \end{cases}$$

Scattered field for $r<a$

$Z_n(kr) = j_n(kr)$

$\sigma_{1n}^{<} = A_{1n} h_n(ka)$

$\tau_{1n}^{<} = B_{1n}[kah_n(ka)]'$

Scattered field for $r>a$

$Z_n(kr) = h_n(kr)$

$\sigma_{1n}^{>} = A_{1n} j_n(ka)$

$\tau_{1n}^{>} = B_{1n}[kaj_n(ka)]'$

Terms

$$\bar{v}_{1n}(\theta) = \frac{P_n^{-1}(\cos\theta)}{\sin\theta} = \frac{-1}{n(n+1)} \frac{P_n^1(\cos\theta)}{\sin\theta}$$

$$\bar{w}_{1n}(\theta) = -\partial_\theta P_n^{-1}(\cos\theta) = \frac{1}{n(n+1)} \partial_\theta P_n^1(\cos\theta)$$

so that the modal coefficients

$$A_{1l} = \frac{ika(2l+1)f_{1l}}{1+\chi_l^\phi} = \frac{-i^l(2l+1)}{h_l(ka)}, \tag{5.5a}$$

$$B_{1l} = \frac{-4ikag_{1l}}{(2l+1)(1+\bar{\chi}_l^\psi)} = \frac{i^l(2l+1)}{[kah_l(ka)]'}. \tag{5.5b}$$

Referring to Eqs. (2.4)–(2.14) and to Table II, this means that (1) for $r\leqslant a$, $\Phi_{1<}^s = -\Phi_{1<}^{\text{inc}}$ and $\Psi_{1<}^s = -\Psi_{1<}^{\text{inc}}$ so that the total potentials, hence the fields, are identically zero there and the boundary conditions $E_{\tan}^s(r=a) = -E_{\tan}^{\text{inc}}(r=a)$ are satisfied and (2) for $r>a$, the standard results for the scattered potentials—fields given, for instance, in Ref. 38, Sec. 6.9, and Ref. 39, Sec. 16.9, are recovered.

VI. CURRENTS ON THE SPHERICAL SHELL

The most stringent test of the dual series solution is the calculation of the currents J_θ and J_ϕ on the open spherical shell. Verification of the required current behavior near the aperture edge is immediately apparent from graphical results. Moreover, the vanishing of the current in the aperture is an excellent test of the results and reflects the satisfaction of the corresponding TE and TM dual series equations in that region. For normal incidence the current expressions (4.11) simply become

$$J_\theta(\theta,\phi) = \left[\frac{-Y_0E_0}{(ka)^2}\right]\cos\phi \sum_{n=1}^{\infty}\left[A_{1n}\frac{P_n^{-1}(\cos\theta)}{\sin\theta} + ikaB_{1n}\,\partial_\theta P_n^{-1}(\cos\theta)\right], \tag{6.1}$$

$$J_\phi(\theta,\phi) = \left[\frac{+Y_0E_0}{(ka)^2}\right]\sin\phi \sum_{n=1}^{\infty}\left[A_{1n}\,\partial_\theta P_n^{-1}(\cos\theta) + ikaB_{1n}\frac{P_n^{-1}(\cos\theta)}{\sin\theta}\right]. \tag{6.2}$$

A. Analytical preconditioning

Consider first the quasistatic case where $ka = 0.01$, $\theta_0 = 120°$. In all of the examples $a = 1.0$. Simply performing the sums in (6.2) with the solution coefficients generated from Eqs. (4.54), we find that the number of terms required to track the square root singularity in J_ϕ is large. The polynomial sum $\Sigma_{n=1}^{L} A_{1n}\,\partial_\theta P_n^{-1}$ is the cause of this difficulty. However, the truncation number N (Sec. IV C) need not be large; and the remaining coefficients $n = N+1,\ldots,L$ are recursively defined from (4.54a) and (4.54b). This is demonstrated in Fig. 3 where the real part of $J_\phi(\theta,\pi/2)[(ka)^2/Y_0E_0]$ is given for various truncation numbers. In Figs. 3(a), 3(b), and 3(c) the truncation numbers $N = 5$ and $L = 50$, 500, and 5000, respectively. However, the results may be improved by treating the singularity analytically as follows.

Inserting the coefficient expressions (4.27a) and (4.41) into (6.1) and (6.2) and referring to the definitions given in Table III, the current components

$$J_\theta = \frac{-Y_0E_0}{2(ka)^2}\cos\phi\left\{\sum_{n=1}^{N}\left[F_{1n}\frac{K_n^E(\theta)}{\sin\theta} + 4ika\frac{G_{1n}}{2n+1}\partial_\theta K_n^H(\theta)\right] - 2ka\xi\left[\frac{K_0^E(\theta)}{\sin\theta} + \partial_\theta K_0^H(\theta)\right]\right\}, \tag{6.3}$$

$$J_\phi = \frac{+Y_0E_0}{2(ka)^2}\sin\phi\left\{\sum_{n=1}^{N}\left[F_{1n}\,\partial_\theta K_n^E(\theta) + 4ika\frac{G_{1n}}{2n+1}\frac{K_n^H(\theta)}{\sin\theta}\right] - 2ka\xi\left[\partial_\theta K_0^E(\theta) + \frac{K_0^H(\theta)}{\sin\theta}\right]\right\} \tag{6.4}$$

result. Two advantages of these expressions are immediate. First, the coefficients obtained from the matrix inversion can be used directly without calculating any additional coefficients by recursion. Second, the currents vanish analytically in the aperture. The terms proportional to F_{1n} and G_{1n} give

Downloaded 21 Nov 2006 to 150.135.222.53. Redistribution subject to AIP license or copyright, see http://jmp.aip.org/jmp/copyright.jsp

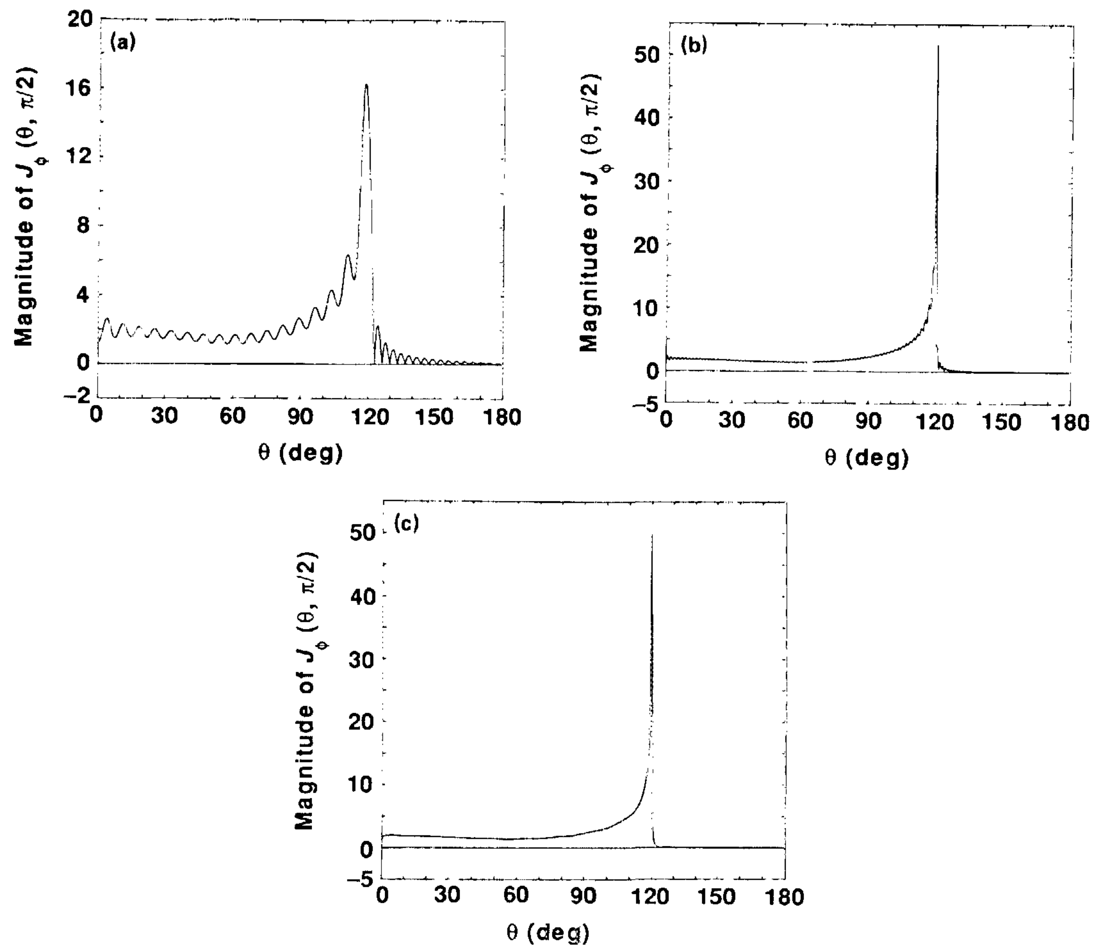

FIG. 3. Brute force summation of the $J_\phi(\theta,\pi/2)$ current expression requires a large number of terms to eliminate the numerical Gibbs' phenomena: (a) $N=5, L=50$; (b) $N=5, L=500$; (c) $N=5, L=5000$.

TABLE III. Special functions and relations for the current expressions.

$$K_0^H(\theta)=\sum_{l=1}^{\infty} L_{1l}^H(\theta_0)P_l^{-1}(\cos\theta)=\begin{cases}+\bar{P}_0^{-1}(\theta) & (\theta_0<\theta\leqslant\pi)\\ +\bar{P}_0^{-1}(\theta)+s_H(\theta) & (0\leqslant\theta<\theta_0)\end{cases}$$

$$K_0^E(\theta)=\sum_{l=1}^{\infty}(2l+1)L_{1l}^E(\theta_0)P_l^{-1}(\cos\theta)=\begin{cases}+\bar{P}_0^{-1}(\theta) & (\theta_0<\theta\leqslant\pi)\\ +\bar{P}_0^{-1}(\theta)+s_E(\theta) & (0\leqslant\theta<\theta_0)\end{cases}$$

$$K_n^H(\theta)=\sum_{l=1}^{\infty}\Gamma_{1,nl}^H(\theta_0)P_l^{-1}(\cos\theta)=\begin{cases}0 & (\theta_0<\theta\leqslant\pi)\\ S_n^H(\theta)+\Lambda_{n0}^H s_H(\theta) & (0\leqslant\theta<\theta_0)\end{cases}$$

$$K_n^E(\theta)=\sum_{l=1}^{\infty}(2l+1)\Gamma_{1,nl}^E(\theta_0)P_l^{-1}(\cos\theta)=\begin{cases}0 & (\theta_0<\theta\leqslant\pi)\\ S_n^E(\theta)+\Lambda_{n0}^E s_E(\theta) & (0\leqslant\theta<\theta_0)\end{cases}$$

where

$$s_H(\theta)=\frac{+4}{\pi\Lambda_{00}^H\sin\theta}\left\{\cos\frac{\theta_0}{2}\left(\cos^2\frac{\theta}{2}-\cos^2\frac{\theta_0}{2}\right)^{1/2}-\cos^2\frac{\theta}{2}\left[\arccos\left(\frac{\cos(\theta_0/2)}{\cos(\theta/2)}\right)\right]\right\}$$

$$s_E(\theta)=\frac{-4}{\pi\Lambda_{00}^E\sin\theta}\left\{\cos\frac{\theta_0}{2}\left(\cos^2\frac{\theta}{2}-\cos^2\frac{\theta_0}{2}\right)^{1/2}+\cos^2\frac{\theta}{2}\left[\arccos\left(\frac{\cos(\theta_0/2)}{\cos(\theta/2)}\right)\right]\right\}$$

$$u_n(\theta)=\frac{4}{\pi}\cos\left(n+\frac{1}{2}\right)\theta_0\frac{[2(\cos\theta-\cos\theta_0)]^{1/2}}{\sin\theta}$$

$$S_n^H(\theta)=\sum_{l=1}^{\infty}\Lambda_{nl}^H P_l^{-1}(\cos\theta)+\Lambda_{n0}^H\bar{P}_0^{-1}(\theta)$$

$$S_n^E(\theta)=u_n(\theta)+(2n+1)S_n^H(\theta)$$

Downloaded 21 Nov 2006 to 150.135.222.53. Redistribution subject to AIP license or copyright, see http://jmp.aip.org/jmp/copyright.jsp

TABLE IV. Derivative relations employed in the current calculations.

$$\partial_\theta s_H(\theta) = \frac{-4}{\pi \Lambda_{00}^H} \left\{ \frac{-\cos\theta}{\sin^2\theta} \left[\cos\frac{\theta_0}{2} \left(\cos^2\frac{\theta}{2} - \cos^2\frac{\theta_0}{2} \right)^{1/2} - \cos^2\frac{\theta}{2} \arccos\left(\frac{\cos(\theta_0/2)}{\cos(\theta/2)} \right) \right] + \frac{1}{2} \arccos\left(\frac{\cos(\theta_0/2)}{\cos(\theta/2)} \right) \right\}$$

$$\partial_\theta s_E(\theta) = \frac{+4}{\pi \Lambda_{00}^E} \left\{ \frac{-\cos\theta}{\sin^2\theta} \left[\cos\frac{\theta_0}{2} \left(\cos^2\frac{\theta}{2} - \cos^2\frac{\theta_0}{2} \right)^{1/2} + \cos^2\frac{\theta}{2} \arccos\left(\frac{\cos(\theta_0/2)}{\cos(\theta/2)} \right) \right] - \frac{1}{2} \arccos\left(\frac{\cos(\theta_0/2)}{\cos(\theta/2)} \right) - \frac{\cos(\theta_0/2)}{2(\cos^2(\theta/2) - \cos^2(\theta_0/2))^{1/2}} \right\}$$

$$\partial_\theta u_n(\theta) = \frac{-8\cos(n+\frac{1}{2})\theta_0}{\pi \sin^2\theta (\cos^2(\theta/2) - \cos^2(\theta_0/2))^{1/2}} \left[\cos^2\frac{\theta}{2} \left(\cos^2\frac{\theta}{2} - \cos^2\frac{\theta_0}{2} \right) + \sin^2\frac{\theta}{2} \cos^2\frac{\theta_0}{2} \right]$$

$$\partial_\theta S_n^H(\theta) = \sum_{l=1}^{\infty} \Lambda_{nl}^H \partial_\theta P_l^{-1} - \Lambda_{n0}^H \frac{\bar{P}_0^{-1}}{\sin\theta}$$

$$\partial_\theta S_n^E(\theta) = \partial_\theta u_n(\theta) + (2n+1)\partial_\theta S_n^H(\theta)$$

no contributions in the aperture because K_n^E and K_n^H are zero there. The terms proportional to ξ also reduce to zero there by (3.9).

Restricting now our attention to the behavior of the current on the metal, (6.3) and (6.4) yield

$$J_\theta = -\frac{Y_0 E_0}{2(ka)^2} \cos\phi \left\{ \sum_{n=1}^{N} \left[F_{1n} \frac{K_n^E(\theta)}{\sin\theta} + 4ika \frac{G_{1n}}{2n+1} \partial_\theta K_n^H(\theta) \right] - 2ka\xi \left[\frac{s_E(\theta)}{\sin\theta} + \partial_\theta s_H(\theta) \right] \right\} \quad (0 \leqslant \theta \leqslant \theta_0), \tag{6.3'}$$

$$J_\phi = +\frac{Y_0 E_0}{2(ka)^2} \sin\phi \left\{ \sum_{n=1}^{N} \left[F_{1n}\, \partial_\theta K_n^E(\theta) + 4ika \frac{G_{1n}}{2n+1} \frac{K_n^H(\theta)}{\sin\theta} \right] - 2ka\xi \left[\partial_\theta s_E(\theta) + \frac{s_H(\theta)}{\sin\theta} \right] \right\} \quad (0 \leqslant \theta \leqslant \theta_0). \tag{6.4'}$$

Near the aperture edge $\theta = \theta_0$ the terms $K_n^E(\theta)$ and $K_n^H(\theta)$ behave, respectively, as $(\theta_0 - \theta)^{1/2}$ and $(\theta_0 - \theta)^{3/2}$. Consequently, the square root singularity in J_ϕ is generated by the term $\partial_\theta K_n^E(\theta)$ and, referring to Table IV, by the term $\partial_\theta s_E(\theta)$. If the former is generated numerically, a large number of coefficients are required. However, referring to

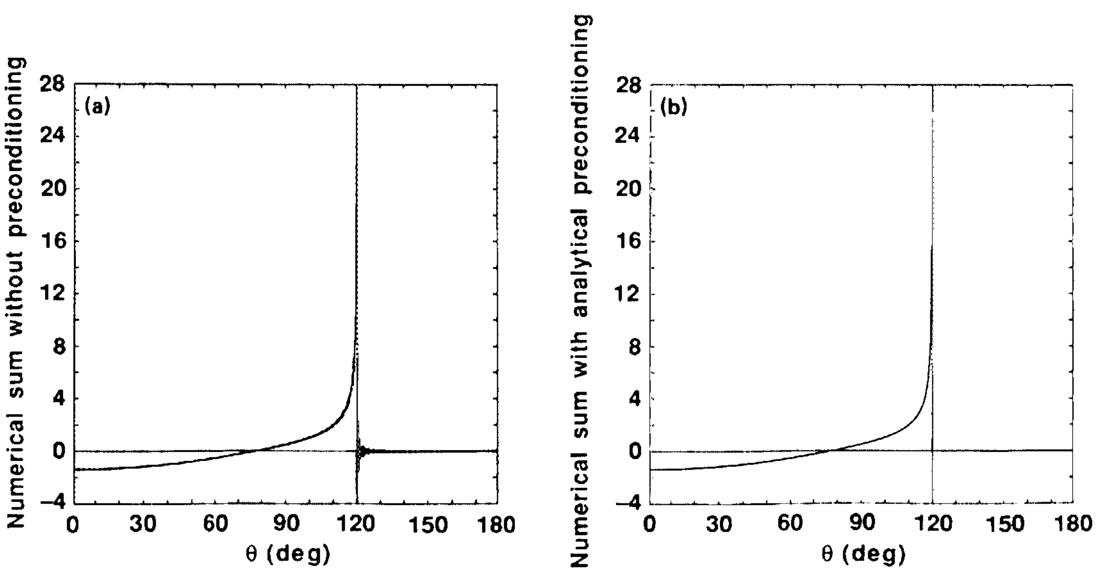

FIG. 4. The Gibbs' phenomena is removed by handling the edge singularity analytically. The dominant sum in the $J_\phi(\theta,\pi/2)$ expression (a) without analytical preconditioning, and (b) with analytical preconditioning.

Downloaded 21 Nov 2006 to 150.135.222.53. Redistribution subject to AIP license or copyright, see http://jmp.aip.org/jmp/copyright.jsp

Tables III and IV for $0 \leqslant \theta < \theta_0$, the relations

$$K_n^E(\theta) = S_n^E(\theta) + \Lambda_{n0}^E s_E(\theta)$$
$$= (2n+1)S_n^H(\theta) + u_n(\theta) + \Lambda_{n0}^E s_E(\theta), \quad (6.5)$$

$$\partial_\theta K_n^E(\theta) = (2n+1)\partial_\theta S_n^H(\theta) + \partial_\theta u_n(\theta) + \Lambda_{n0}^E\, \partial_\theta s_E(\theta) \quad (6.6)$$

indicate that one only needs to evaluate $S_n^H(\theta)$ and $\partial_\theta S_n^H(\theta)$ numerically. Since $S_n^H(\theta) = K_n^H(\theta) - \Lambda_{n0}^H s_H(\theta)$ over the metal and near the aperture edge $\partial_\theta K_n^H(\theta) \sim (\theta_0 - \theta)^{1/2}$ and $\partial_\theta s_H \sim (\theta_0 - \theta)^{1/2}$, the term $\partial_\theta S_n^H(\theta) \sim (\theta_0 - \theta)^{1/2}$ near $\theta = \theta_0$, which circumvents the numerical difficulties. The square root singularity is handled analytically through the terms $\partial_\theta u_n$ and $\partial_\theta s_E$. A comparison of $\partial_\theta K_1^E(\theta)$ evaluated directly and with (6.6) is given in Fig. 4. Each sum included 800 terms. As desired, the (numerical) oscillations were removed by the analytical preconditioning.

B. Numerical results

Because the current components

$$J_\theta(\theta,\phi) = J_\theta(\theta,0)\cos\phi, \quad (6.7)$$

$$J_\phi(\theta,\phi) = J_\phi(\theta,\pi/2)\sin\phi, \quad (6.8)$$

their important features are illustrated succinctly by considering $J_\theta(\theta,0)$ and $J_\phi(\theta,\pi/2)$. Examples of the scaled current terms $\mathscr{J}_\theta = J_\theta(\theta,0)[-2(ka)^2/Y_0E_0]$ and $\mathscr{J}_\phi = J_\phi(\theta,\pi/2)[2(ka)^2/Y_0E_0]$ are given in Figs. 5–10 for various ka, aperture sizes, and angles of incidence.

Values of $|\mathscr{J}_\theta|$ and $|\mathscr{J}_\phi|$ are given in Figs. 5 and 6 for the quasistatic limit ($ka = 0.01$), the angle of incidence $\theta^{\text{inc}} = 0.0$, and, respectively, the aperture angles $\theta_0 = 120°$ and $\theta_0 = 170°$. For both cases the truncation number $N = 10$. Essentially the same results were generated with $N = 3$. This low truncation number is typical for quasistatic cases because the $n = 1$ term dominates the behavior. The term $|\mathscr{J}_\theta|$ is given in Fig. 7 for $\theta^{\text{inc}} = 0.0$, $\theta_0 = 120°$, and the ka values 1.0, 3.0, 5.0, and 10.0. The corresponding graphs of $|\mathscr{J}_\phi|$ are given in Fig. 8. For all of these cases the truncation number was taken to be $N = 10(ka)$. This choice yields convergent results. The plots in Fig. 7 clearly demonstrate that our solution reproduces the required $(\theta_0 - \theta)^{1/2}$ behavior of J_θ near $\theta = \theta_0$; Fig. 8 demonstrates that the required square root singularity of J_ϕ near $\theta = \theta_0$ is present. In Fig. 9 the terms $\text{Re}(\mathscr{J}_\theta)$ and $|\mathscr{J}_\theta|$ are plotted for $\theta_0 = 120°$, $ka = 1.0$, $\theta^{\text{inc}} = 0°$, and $\theta^{\text{inc}} = 180°$. Very different behaviors are obtained. When the wave is incident on the shell

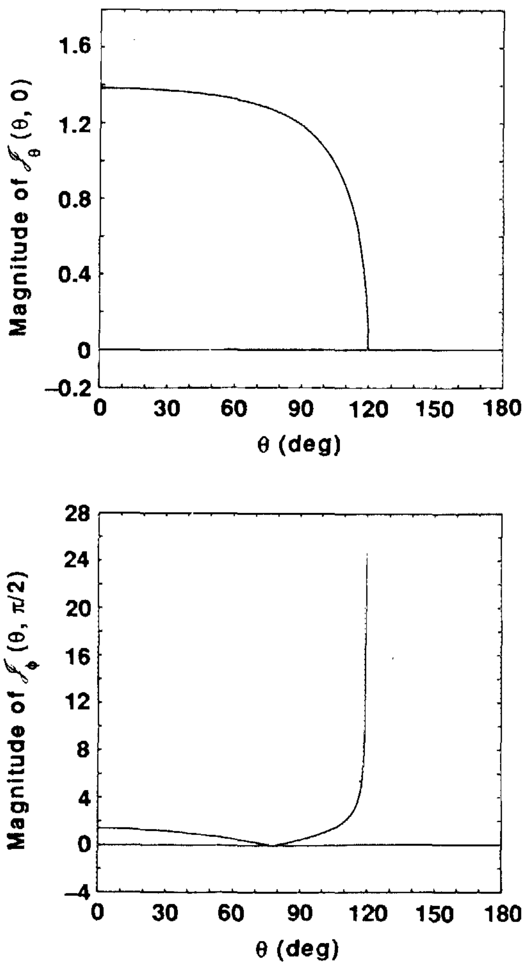

FIG. 5. The magnitudes of the current terms $\mathscr{J}_\theta(\theta,0)$ and $\mathscr{J}_\phi(\theta,\pi/2)$ induced on an open spherical shell with $\theta_0 = 120°$ when $ka = 0.01$ and $\theta^{\text{inc}} = 0.0°$.

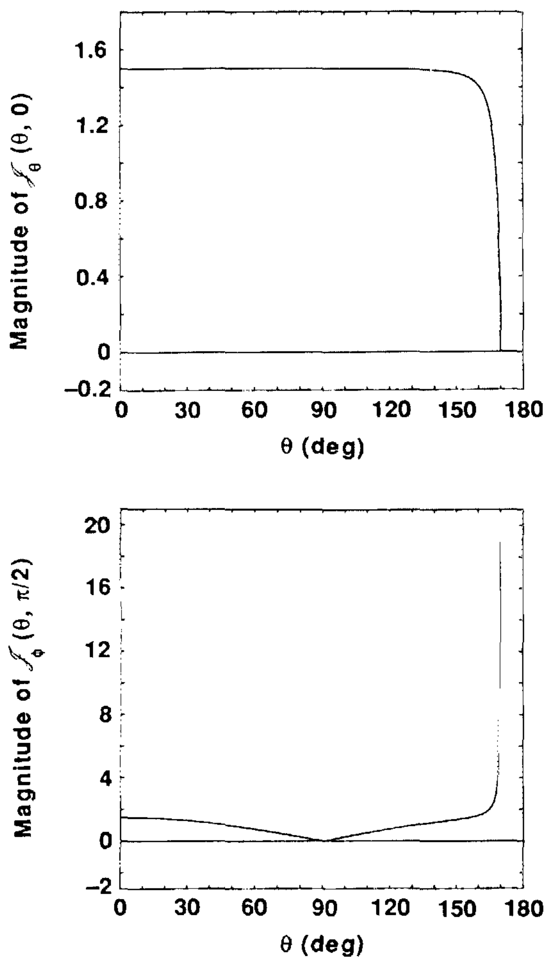

FIG. 6. The magnitudes of the current terms $\mathscr{J}_\theta(\theta,0)$ and $\mathscr{J}_\phi(\theta,\pi/2)$ induced on an open spherical shell with $\theta_0 = 170°$ when $ka = 0.01$ and $\theta^{\text{inc}} = 0.0°$.

Downloaded 21 Nov 2006 to 150.135.222.53. Redistribution subject to AIP license or copyright, see http://jmp.aip.org/jmp/copyright.jsp

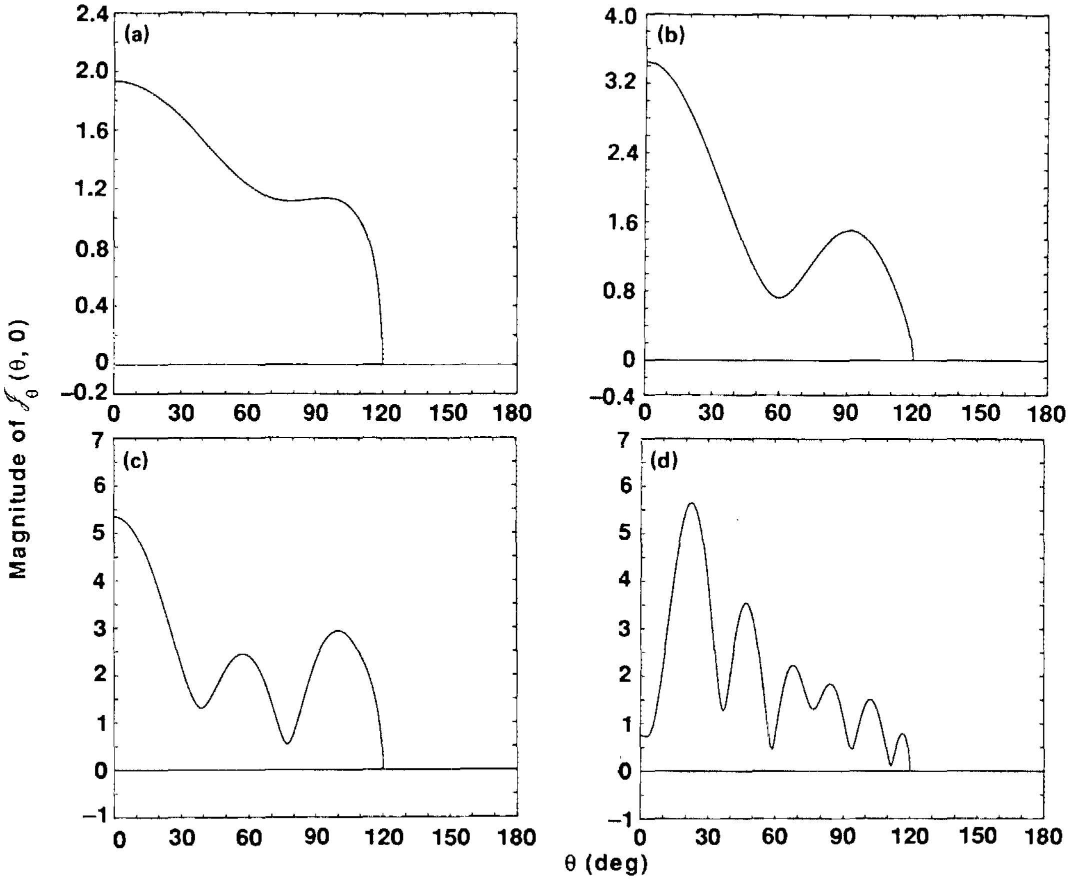

FIG. 7. The current term $\mathscr{J}_\theta(\theta,0)$ induced on an open spherical shell with $\theta_0 = 120°$ when $\theta^{\rm inc} = 0°$ and the ka of the incident plane wave is (a) 1.0, (b) 3.0, (c) 5.0, and (d) 10.0.

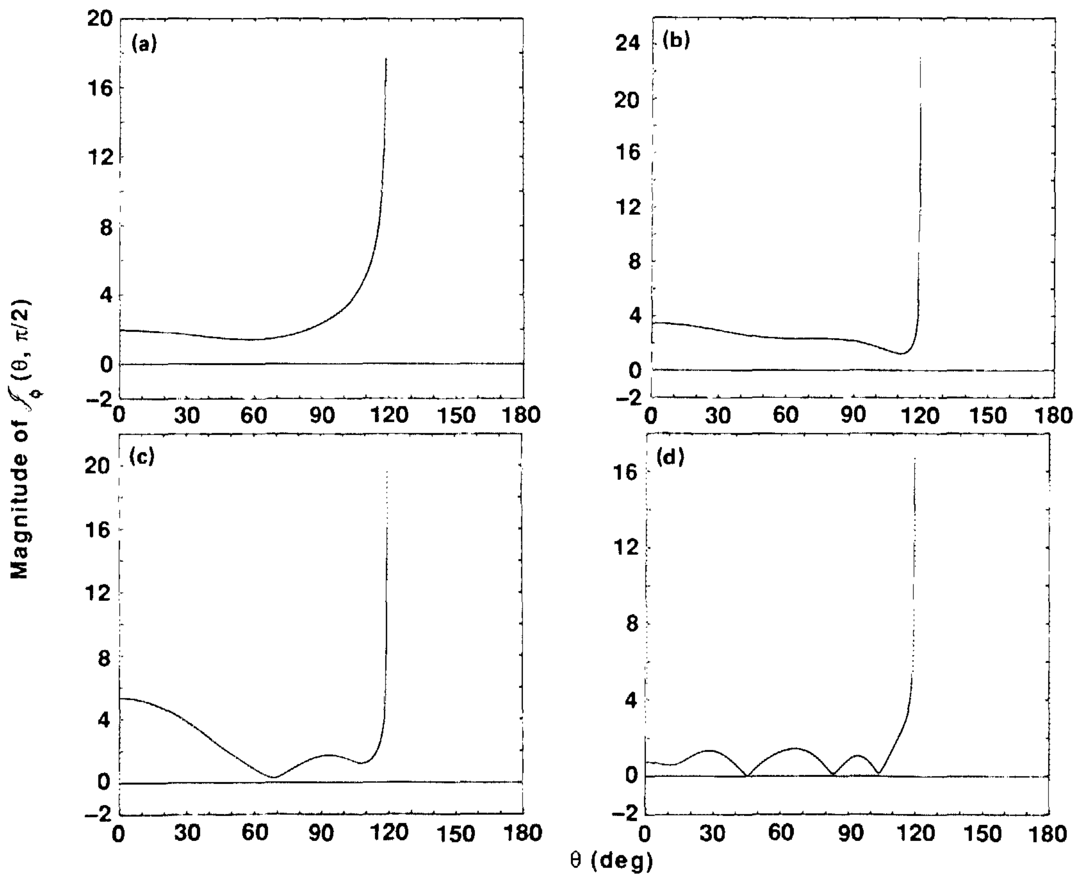

FIG. 8. The current term $\mathscr{J}_\phi(\theta,\pi/2)$ induced on an open spherical shell with $\theta_0 = 120°$ when $\theta^{\rm inc} = 0°$ and the ka of the incident plane wave is (a) 1.0, (b) 3.0, (c) 5.0, and (d) 10.0.

Downloaded 21 Nov 2006 to 150.135.222.53. Redistribution subject to AIP license or copyright, see http://jmp.aip.org/jmp/copyright.jsp

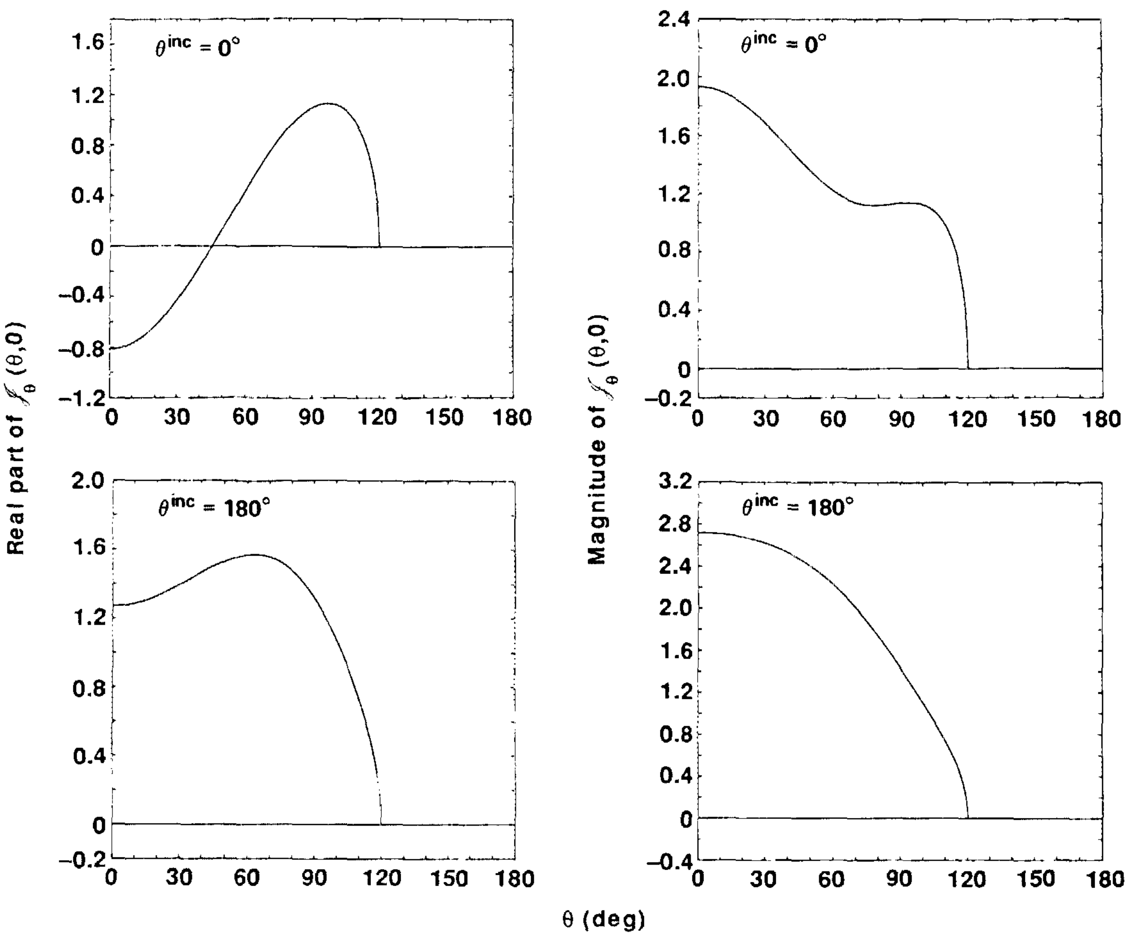

FIG. 9. A comparison of the real part and the magnitude of the current term $\mathscr{J}_\theta(\theta,0)$ induced on an open spherical shell with $\theta_0 = 120°$ when $ka = 1.0$ and the angle of incidence $\theta^{\rm inc} = 0°$ and $\theta^{\rm inc} = 180°$.

($\theta^{\rm inc} = 180°$), $|\mathscr{J}_\theta|$ is much more uniformly distributed over the shell. The hump near the aperture edge which appeared when $\theta^{\rm inc} = 0°$ is no longer present. In Fig. 10, $|\mathscr{J}_\theta|$ is given for $\theta^{\rm inc} = 0°$ and $ka = 1.0$ when $\theta_0 = 120°$ and $\theta_0 = 170°$. The latter case exhibits a more pronounced hump near the aperture edge.

The distributions of J_θ and J_ϕ over the entire spherical shell for $ka = 3$, $\theta^{\rm inc} = 0°$, and $\theta_0 = 120°$ are shown in Figs. 11 and 12. In Fig. 11 the values of $|\mathscr{J}_\theta|$ and $|\mathscr{J}_\phi|$ are replotted in more detail to provide a reference for Figs. 12. In Figs. 12(a) and 12(b) $\mathscr{J}_\theta$ is viewed from the directions ($\theta = 0$, $\phi = 0$) and ($\theta = 76°$, $\phi = 125°$). Dark red represents the largest values; dark blue the smallest ones. The characteristic cosine pattern and null at the aperture edge are very apparent. The corresponding views of $\mathscr{J}_\phi$ are given in Figs. 12(c) and 12(d). The associated sine pattern and edge singularity are nicely reproduced.

The current results have been validated with a totally independent method[19]: a completely numerical solution based upon a method of moments (MoM) analysis of the problem. It has been demonstrated that the MoM solution converges to the dual series results when the former is applicable.

VII. ENERGY DENSITIES

To provide some measure of the degree of coupling of the incident field into the spherical cavity, the energy density at the center of the shell normalized to the incident field energy density there was calculated. This also allows a direct comparison with Senior–Desjardins results.[12,13]

Consider the normal incidence field expressions given in Table II for $r = 0$. With the small argument relations in the Appendix, one obtains ($n \neq 0$)

$$j_n(0) \equiv 0, \quad \{[x j_n(x)]'/x\}_{x=0} = \tfrac{2}{3}\delta_{n1},$$
$$[j_n(x)/x]_{x=0} = \tfrac{1}{3}\delta_{n1}.$$

Moreover, $P_1^{-1}(\cos\theta)/\sin\theta = -\frac{1}{2}$ and $-\partial_\theta P_1^{-1}(\cos\theta) = \cos(\theta/2)$. Therefore, the general electric and magnetic field vectors at the origin are

$$(E_r,E_\theta,E_\phi)(r=0) = (i/3)E_0\tau_{11}(\sin\theta\cos\phi, \cos\theta\cos\phi, -\sin\phi), \quad (7.1)$$

$$(H_r,H_\theta,H_\phi)(r=0) = (i/3)Y_0E_0\sigma_{11}(\sin\theta\sin\phi, \cos\theta\sin\phi, +\cos\phi), \quad (7.2)$$

Downloaded 21 Nov 2006 to 150.135.222.53. Redistribution subject to AIP license or copyright, see http://jmp.aip.org/jmp/copyright.jsp

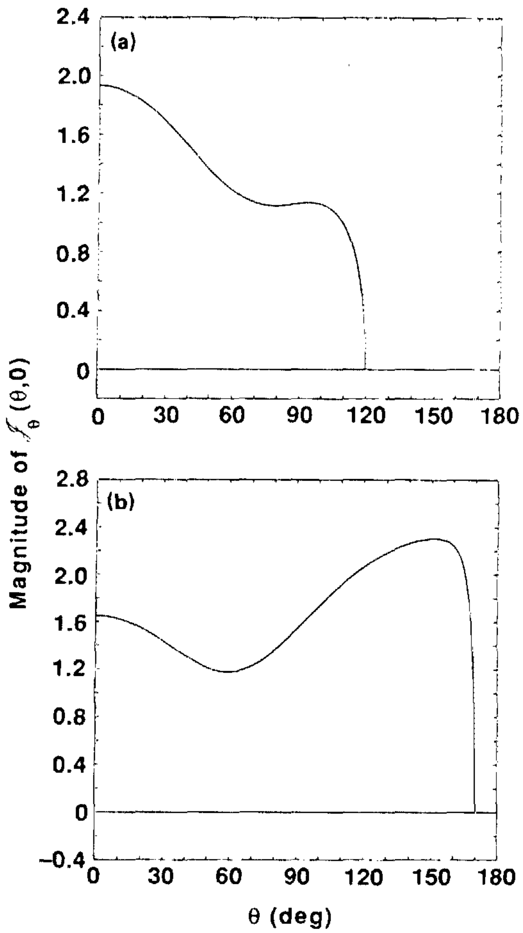

FIG. 10. A comparison of the magnitudes of the current term $\mathcal{J}_\theta(\theta,0)$ induced on open spherical shells with (a) $\theta_0 = 120°$ and (b) $\theta_0 = 170°$, when $ka = 1.0$ and the angle of incidence $\theta^{\text{inc}} = 0°$.

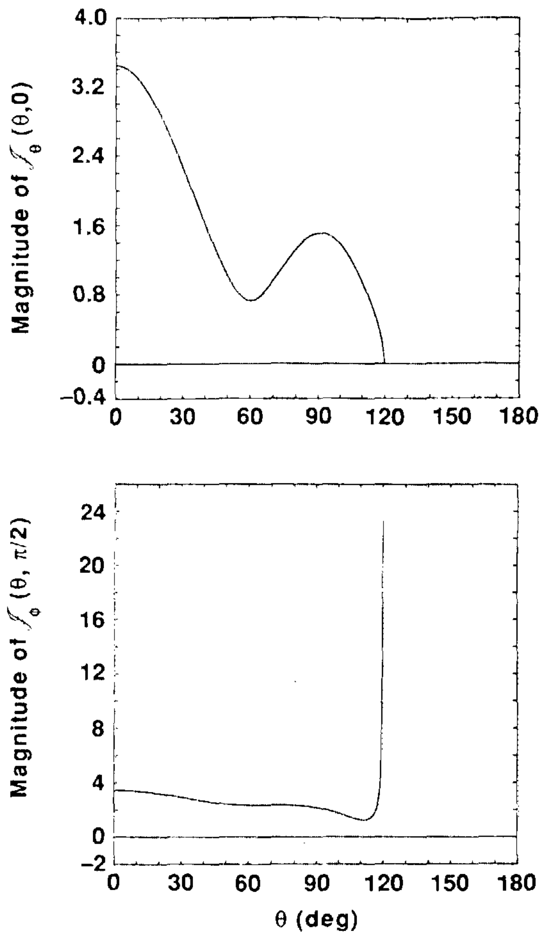

FIG. 11. The magnitudes of the current terms $\mathcal{J}_\theta(\theta,0)$ and $\mathcal{J}_\theta(\theta,\pi/2)$ induced on an open spherical shell with $\theta_0 = 120°$ when $ka = 3.0$ and the angle of incidence $\theta^{\text{inc}} = 0°$.

where

$$\sigma_{11} = \sigma_{11}^{\text{inc}} + \sigma_{11}^{<} = \sigma_{11}^{\text{inc}} + A_{11}h_1(ka), \tag{7.3}$$

$$\tau_{11} = \tau_{11}^{\text{inc}} + \tau_{11}^{<} = \tau_{11}^{\text{inc}} + B_{11}[kah_1(ka)]', \tag{7.4}$$

the incident field terms being

$$\sigma_{11}^{\text{inc}} = \begin{cases} 3i, & \theta^{\text{inc}} = 0, \\ 3i, & \theta^{\text{inc}} = \pi, \end{cases} \tag{7.5}$$

$$\tau_{11}^{\text{inc}} = \begin{cases} -3i, & \theta^{\text{inc}} = 0, \\ 3i, & \theta^{\text{inc}} = \pi. \end{cases} \tag{7.6}$$

Consequently, the associated energy density relation is simply

$$\begin{aligned} U(r=0) &= \tfrac{1}{2}(|\mathbf{E}|^2 + |Z_0\mathbf{H}|^2)(r=0) \\ &= E_0^2(|\sigma_{11}|^2 + |\tau_{11}|^2)/18, \end{aligned} \tag{7.7}$$

which leads to the desired energy density ratio

$$\begin{aligned} \frac{U_{\text{tot}}(r=0)}{U_{\text{inc}}(r=0)} &= \frac{|\sigma_{11}^{\text{inc}} + \sigma_{11}^{<}|^2 + |\tau_{11}^{\text{inc}} + \tau_{11}^{<}|^2}{|\sigma_{11}^{\text{inc}}|^2 + |\tau_{11}^{\text{inc}}|^2} \\ &= \tfrac{1}{18}\{|3i + A_{11}h_1(ka)|^2 + |3i \mp B_{11}[kah_1(ka)]'|^2\} \\ &= \tfrac{1}{2}\{|1 - (i/3)A_{11}h_1(ka)|^2 + |1 \\ &\quad \pm (i/3)B_{11}[kah_1(ka)]'|^2\}. \end{aligned} \tag{7.8}$$

The upper sign is appropriate for $\theta^{\text{inc}} = 0$; the lower sign for $\theta^{\text{inc}} = \pi$.

The quantity $10\log_{10}[U_{\text{tot}}(r=0)/U_{\text{inc}}(r=0)]$ is plotted in Figs. 13–15 for the aperture angles 10°, 30°, and 60° (i.e., for $\theta_0 = 170°$, 150°, and 120°) and for the angle of incidence $\theta^{\text{inc}} = 0°$. Several interesting features are apparent immediately. For $\theta_0 = 170°$ the open spherical shell acts very similarly to a spherical cavity of the same size. The peaks in the data at $ka = 4.49$, 2.74, 3.87, and 4.97 closely correspond, respectively, to the lowest TE and TM modes of a closed cavity (see Ref. 36, pp. 268–271); i.e., to the lowest-order zero x_{11} of $[xj_1(x)]$ and to the zeros x'_{11}, x'_{12}, and x'_{13} of $[xj_1(x)]'$. They are slightly offset (detuned) from the closed cavity values because of the presence of the aperture. Extensions of the discussion in Sec. V for θ_0 near π and for ka small lead to the approximate coefficient expressions in this ka region,

$$A_{11}h_1(ka) - \frac{\sum_{n=1}^{N} f_{1n}\Gamma_{n1}^{E}}{j_1(ka)}, \tag{7.9a}$$

$$B_{11}[kah_1(ka)]' - \frac{\sum_{n=1}^{N}(3g_{1n}\Gamma_{n1}^{H}/2n+1)}{[kaj_1(ka)]'}, \tag{7.9b}$$

which readily explain the locations of the observed features. At higher ka peaks corresponding to the roots x_{np} of

Downloaded 21 Nov 2006 to 150.135.222.53. Redistribution subject to AIP license or copyright, see http://jmp.aip.org/jmp/copyright.jsp

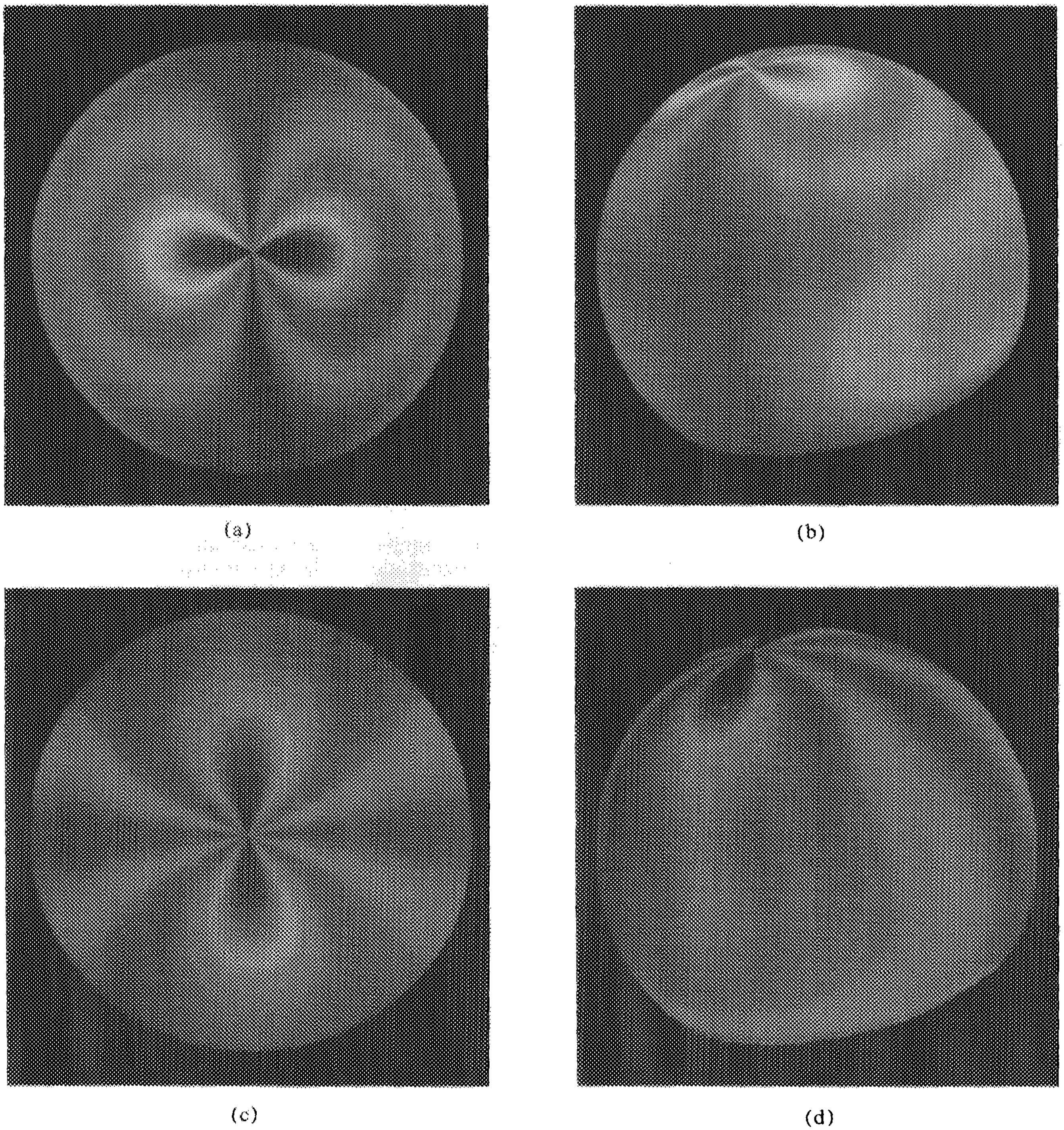

FIG. 12. The modal structure of the currents induced on an open spherical shell with $\theta_0 = 120°$ when $ka = 3.0$ and the angle of incidence $\theta^{\rm inc} = 0°$ is revealed with three dimensional graphics: (a) a top view of the magnitude of the current term $\mathscr{J}_\theta(\theta,\phi)$; (b) a side view of the magnitude of the current term $\mathscr{J}_\theta(\theta,\phi)$; (c) a top view of the magnitude of the current term $\mathscr{J}_\phi(\theta,\phi)$; (d) a side view of the magnitude of the current term $\mathscr{J}_\phi(\theta,\phi)$.

$[xj_n(x)] = 0$ and x'_{np} of $[xj_n(x)]' = 0$ appear. The antiresonance form of the peaks at $ka = 3.87$ and 4.97 was not anticipated. In fact, only the TE_{n1} and TM_{n1} modes ($n = 1,2,...$) develop the resonance form of the peaks; all others have the antiresonant form. This behavior is a result of (1) the modal patterns induced in the open cavity—all TE_{np} and TM_{np} ($p \neq 1$) modes have nulls at $r = 0$, and (2) a reradiation effect that occurs because the aperture is backed by a resonant cavity.[40] The important features in the ka scans of (7.8) for larger apertures are associated with the modes effecting the antiresonant behavior.

Detuning of the cavity by the larger aperture is noticeable in the $\theta_0 = 150°$ data. The resonance peaks are broadened and the antiresonance peaks have become broad depressions. The resonance locations are downshifted to lower ka values (lower frequency); the antiresonance locations are

Downloaded 21 Nov 2006 to 150.135.222.53. Redistribution subject to AIP license or copyright, see http://jmp.aip.org/jmp/copyright.jsp

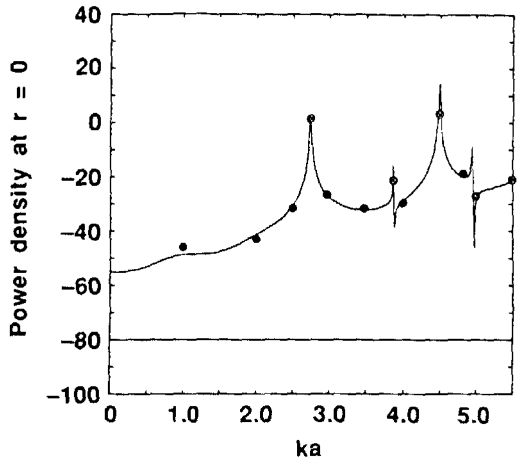

FIG. 13. A scan in ka of the total energy density of the field at the origin normalized to the energy density of the incident field there for an open spherical shell having an aperture angle of 170° and a plane wave incident at $\theta^{inc} = 0°$. The solid line is generated by the dual series solution, the dots by a MoM surface patch code.

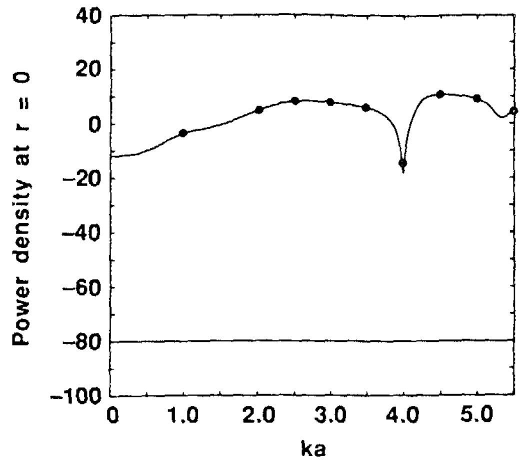

FIG. 15. A scan in ka of the total energy density of the field at the origin normalized to the energy density of the incident field there for an open spherical shell having an aperture angle of 120° and a plane wave incident at $\theta^{inc} = 0°$. The solid line is generated by the dual series solution, the dots by a MoM surface patch code.

upshifted to higher ka values (higher frequency). The depressions at the antiresonance locations indicate that this slightly open cavity may have poor energy storage characteristics, hence a large scattering cross section at those points. Energy storage and cross-section calculations are also in progress to study this (for instance see Ref. 40).

The largest aperture ($\theta_0 = 120°$) data shows nearly a complete detuning of the cavity. The observed depressions are shallower and broadened. They correspond to the original antiresonance locations $ka = 3.87$ and 4.97, thus demonstrating the considerable upshift in ka of their locations as the aperture size increases. The data also indicates a focusing of the energy near $r = 0$ over a large range of ka. This is expected since the shell is beginning to look largely like a spherical reflector when $\theta_0 = 120°$.

Comparing these results with those of Senior and Desjardins, very distinct dissimilarities are evident. Although the resonance peaks at $ka = 2.74$ and 4.49 are present in their results, the antiresonance peaks at $ka = 3.87$ and 4.97 are not. Similarly, the antiresonance depressions in the $\theta_0 = 150°$ data are absent. Also, the levels they predicted for small ka are close to 50 dB smaller in the $\theta_0 = 170°$ data and 20 dB smaller in the $\theta_0 = 150°$ data than ours. Analogously, their resonance peak levels are higher than those we predict. Our results again have been validated with a method of moments calculation.[19] Sample data points from those checks have been included in Figs. 13–15. Agreement is very good.

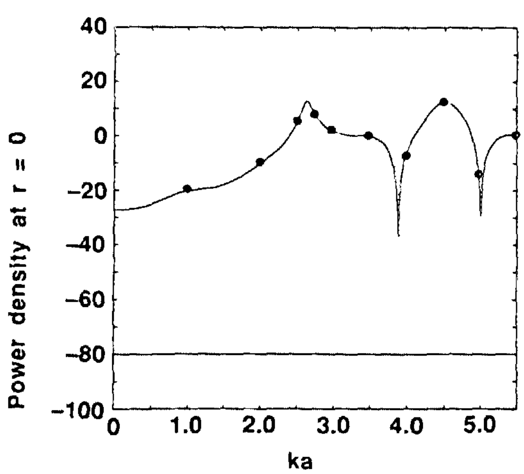

FIG. 14 A scan in ka of the total energy density of the field at the origin normalized to the energy density of the incident field there for an open spherical shell having an aperture angle of 150° and a plane wave incident at $\theta^{inc} = 0°$. The solid line is generated by the dual series solution, the dots by a MoM surface patch code.

VIII. SUMMARY

A complete solution of the scattering of a plane wave from a spherical shell having a circular aperture was developed in this paper. The angle of incidence and the polarization of the plane wave were arbitrary. This solution was constructed with a dual series equations approach and was validated in several different ways. Numerical results were given for the case of normal incidence. Induced currents on the open spherical shell were presented and it was demonstrated that they satisfy Meixner's edge conditions. Energy density scans in ka were also given; they were dominated by resonance features characteristic of the open spherical cavity.

Several new concepts and techniques were reported. The associated Legendre functions P_n^{-m} for $0 \leqslant n < m$ and their duals $\bar{P}_n^{-m}$ were introduced to produce a system of pseudodecoupled TE and TM dual series equations and to insure satisfaction of Meixner's edge conditions. Procedures were described in detail that generated an analytical solution of the resulting, previously untreated dual series systems and a numerical solution of the resulting infinite system of linear equations for the modal coefficients. Analytical preconditioning of the current sums led to results free of any Gibbs oscillations. The resonance features in the ka scans of an energy density ratio at the origin were observed to be predominantly of an antiresonant form.

Cross-section and stored energy calculations are currently in progress. Preliminary cross-section results are also dominated by antiresonance features and suggest that they

Downloaded 21 Nov 2006 to 150.135.222.53. Redistribution subject to AIP license or copyright, see http://jmp.aip.org/jmp/copyright.jsp

are characteristic of a cavity-backed aperture. These studies are summarized in Ref. 40.

ACKNOWLEDGMENTS

The authors would like to extend special thanks to Art Gautesen of the Department of Mathematics at Iowa State University and to Larry Warne at Sandia National Laboratories for a variety of thoughts and discussions that led to the successful conclusion of our work. The authors would also like to thank Brian Cabral of the Computer Systems Research Group at Lawrence Livermore National Laboratory for developing the graphics package that created the three-dimensional color figures.

This work was performed by the Lawrence Livermore National Laboratory and Sandia National Laboratories under the auspices of the U. S. Department of Energy under Contracts No. W-7405-ENG-48 and DE-AC04-76DP00789, respectively.

APPENDIX: ASYMPTOTIC BEHAVIOR OF THE TERMS χ_n^ϕ AND χ_n^ψ

The small argument and large index behavior of the terms χ_n^ϕ and χ_n^ψ will be developed for $n>0$. The spherical Bessel function expansions (see Ref. 37, Eqs. 10.1.2 and 10.1.3)

$$j_n(x)=\frac{(\pi/4)^{1/2}(x/2)^n}{\Gamma(n+\frac{3}{2})}\times\left[1-\frac{x^2}{2(2n+3)}+\mathscr{O}\left(\frac{x^4}{n^2}\right)\right], \tag{A1}$$

$$h_n(x)=\frac{-i}{(4\pi)^{1/2}}\left(\frac{x}{2}\right)^{-(n+1)}\Gamma\left(n+\frac{1}{2}\right)\times\left[1+\frac{x^2}{2(2n-1)}+\mathscr{O}\left(\frac{x^4}{n^2}\right)\right], \tag{A2}$$

and the identity

$$\Gamma(n+\tfrac{1}{2})=\{[(2n-1)\cdot\cdots\cdot 5\cdot 3\cdot 1]/2^n\}\pi^{1/2} \tag{A3}$$

provide the necessary expressions. Equations (A1) and (A2) yield

$$[xj_n(x)]'=\left(\frac{\pi}{4}\right)^{1/2}\frac{(n+1)}{\Gamma(n+\frac{3}{2})}\left(\frac{x}{2}\right)^n\times\left[1-\frac{(n+3)x^2}{2(n+1)(2n+3)}+\mathscr{O}\left(\frac{x^4}{n^2}\right)\right], \tag{A4}$$

$$[xh_n(x)]'=\frac{i}{(4\pi)^{1/2}}n\Gamma\left(n+\frac{1}{2}\right)\left(\frac{x}{2}\right)^{-(n+1)}\times\left[1+\frac{(n-2)x^2}{2n(2n-1)}+\mathscr{O}\left(\frac{x^4}{n^2}\right)\right]. \tag{A5}$$

Combining (A1)–(A3) gives

$$j_n(x)h_n(x)=\frac{1}{i(2n+1)x}\times\left[1+\frac{2x^2}{(2n-1)(2n+3)}+\mathscr{O}\left(\frac{x^4}{n^4}\right)\right]; \tag{A6}$$

combining (A3)–(A5) gives

$$[xj_n(x)]'[xh_n(x)]'=\frac{n(n+1)}{-i(2n+1)x}\times\left[1-\frac{(2n^2+2n+3)x^2}{n(n+1)(2n-1)(2n+3)}+\mathscr{O}\left(\frac{x^4}{n^4}\right)\right]. \tag{A7}$$

Consequently, for small arguments

$$\lim_{x\to 0}\chi_n^\phi=\lim_{x\to 0}\{[i(2n+1)xj_n(x)h_n(x)]-1\}\sim 0, \tag{A8}$$

$$\lim_{x\to 0}\chi_n^\psi=\lim_{x\to 0}\left[\left\{\frac{-i(2n+1)x}{n(n+1)}\times[xj_n(x)]'[xh_n(x)]'\right\}-1\right]\sim 0, \tag{A9}$$

and for indices larger than the argument

$$\lim_{n\to\infty}\chi_n^\phi(x)=\lim_{n\to\infty}\mathscr{O}(x^2/n^2)\sim 0, \tag{A10}$$

$$\lim_{n\to\infty}\chi_n^\psi(x)=\lim_{n\to\infty}\mathscr{O}(x^2/n^2)\sim 0. \tag{A11}$$

Note that this limiting behavior is responsible for the number of terms required for convergence of the solution. In particular, for large enough N, the terms

$$\chi_N^\phi(ka)\sim\chi_N^\psi(ka)\sim(ka/N)^2$$

and the elements of the matrix $\mathscr{M}_{ij}$ in (4.49) are small. This explains the choice $N=10\,ka$ for the examples.

[1]A. M. Radin and V. P. Shestopalov, USSR Comp. Math. Math. Phys. **14**(5), 137 (1974).
[2]A. M. Radin and V. P. Shestopalov, Sov. Phys. Dokl. **18**, 642 (1974).
[3]A. M. Radin, V. A. Rezunenko, and V. P. Shestopalov, USSR Comp. Math. Math. Phys. **17**(2), 104 (1977).
[4]S. S. Vinogradov and V. P. Shestopalov, Sov. Phys. Dokl. **22**, 638 (1977).
[5]S. S. Vinogradov, Yu A. Tuchkin, and V. P. Shestopalov, Sov. Phys. Dokl. **23**, 650 (1978).
[6]S. S. Vinogradov, Yu A. Tuchkin, and V. P. Shestopalov, Sov. Phys. Dokl. **25**, 531 (1980).
[7]S. S. Vinogradov, Yu A. Tuchkin, and V. P. Shestopalov, Sov. Phys. Dokl. **26**, 169 (1981).
[8]S. S. Vinogradov and V. P. Shestopalov, Sov. Phys. Dokl. **26**, 314 (1981).
[9]S. S. Vinogradov, Radiophys. Quantum Electron. **26**, 78 (1983).
[10]K. F. Casey, Proceedings of the National Radio Science Meeting, June 1981, p. 69.
[11]S. Chang and T. B. A. Senior, U. S. Air Force Weapons Lab. Interaction Note 141, Albuquerque, NM, April 1969.
[12]T. B. A. Senior and G. A. Desjardins, U. S. Air Force Weapons Lab. Interaction Note 142, Alburquerque, NM, August 1973.
[13]T. B. A. Senior and G. A. Desjardins, IEEE Trans. Electromag. Compat. **EMC-16**, 205 (1974).
[14]T. B. A. Senior, U. S. Air Force Weapons Lab. Interaction Note 220, Albuquerque, NM, January 1975.
[15]R. K. Jones and T. H. Shumpert, IEEE Trans. Antennas Propagat. **AP-28**, 128 (1980).
[16]J. Meixner, Nachr. Akad. Wiss. Gottingen **2**, 74 (1946).
[17]J. Meixner, A. Naturforsch. **3a**, 506 (1948).
[18]R. W. Ziolkowski and W. A. Johnson, Radio Sci. **22**, 169 (1987).
[19]W. A. Johnson and R. W. Ziolkowski, Proceedings of the National Radio Science Meeting, June 1984, p. 174.
[20]W. A. Johnson and R. W. Ziolkowski, Radio Sci. **19**, 275 (1984).
[21]R. W. Ziolkowski, W. A. Johnson, and K. F. Casey, Radio Sci. **19**, 1425 (1984).

Downloaded 21 Nov 2006 to 150.135.222.53. Redistribution subject to AIP license or copyright, see http://jmp.aip.org/jmp/copyright.jsp

[22]R. W. Ziolkowski, SIAM J. Math. Anal. **16**, 358 (1985).
[23]R. W. Ziolkowski and J. B. Grant, to be published in IEEE Trans. Antennas Propaga.
[24]R. W. Ziolkowski and J. B. Grant, IEEE Trans. Microwave Theor. Tech. **MTT-34**, 1164 (1986).
[25]R. W. Ziolkowski and W. A. Johnson, UCRL-92940, Lawrence Livermore National Laboratory, Livermore, CA, July 1985.
[26]D. S. Jones, *The Theory of Electromagnetism* (Pergamon, New York, 1964).
[27]M. Born and E. Wolf, *Principles of Optics* (Macmillan, New York, 1964), 2nd ed.
[28]C. H. Wilcox, J. Math. Mech. **6**, 167 (1957).
[29]C. J. Bouwkamp and H. B. G. Casimir, Physica **20**, 539 (1954).
[30]J. H. Bruning and Y. T. Lo, IEEE Trans. Antennas Propagat. **AP-19**, 378 (1971); **AP-19**, 391 (1971).
[31]C. Liang and Y. T. Lo, Radio Sci. **2**, 1481 (1967).
[32]I. S. Gradshteyn and I. M. Ryzhik, *Table of Integrals, Series, and Products* (Academic, New York, 1965).
[33]T. M. MacRobert, *Spherical Harmonics* (Pergamon, New York, 1967), 3rd ed.
[34]E. W. Hobson, *The Theory of Spherical and Ellipsoidal Harmonics* (Chelsea, New York, 1955).
[35]L. Robin, *Fonctions Spheriques de Legendre et Fonctions Spheroidales* (Gauthier-Villars, Paris, 1958).
[36]F. Oberhettinger, *Fourier Expansions: A Collection of Formulas* (Academic, New York, 1973).
[37]*Handbook of Mathematical Functions*, edited by M. Abramowitz and I. A. Stegun (Dover, New York, 1970).
[38]R. F. Harrington, *Time-Harmonic Electromagnetic Fields* (McGraw-Hill, New York, 1977).
[39]J. D. Jackson, *Classical Electrodynamics* (Wiley, New York, 1962).
[40]R. W. Ziolkowski, to be published in Radio Sci.

Downloaded 21 Nov 2006 to 150.135.222.53. Redistribution subject to AIP license or copyright, see http://jmp.aip.org/jmp/copyright.jsp